Title

Modeling energy dissipation and hydraulic jump regime responses to channel nonuniformity at river steps

Journal

Journal of Geophysical Research: Earth Surface, 113(3)

ISSN

2169-9003

Authors

Wrick, JR
Pasternack, GB

Publication Date

2008-09-24

DOI

10.1029/2007JF000873

Peer reviewed

Title: Modeling energy dissipation and hydraulic jump regime responses to channel non-uniformity at river steps

Running Title: River step hydraulics

Authors: Joshua R. Wyrick[1,2] and Gregory B. Pasternack[1,*]

Addresses:

[1]Department of Land, Air, and Water Resources, University of California, One Shields Avenue, Davis, Ca 95616, USA

[2]Current Address: Civil and Environmental Engineering Department, Rowan University, 201 Mullica Hill Rd., Glassboro, NJ, 08071, USA

*Corresponding author

Cite as: Wyrick, J. R. and Pasternack, G. B. 2008. Modeling energy dissipation and hydraulic jump regime responses to channel nonuniformity at river steps. Journal of Geophysical Research 113, F03003, doi:10.1029/2007JF000873.

Abstract

The river step is an important driver for geomorphic evolution in bedrock rivers, but the effect that variations in channel geometry upstream and downstream of a river step have on hydraulic jump regime and energy dissipation has not previously been investigated. The associated hydraulic jump is inherent to a river step and its regime is a primary control on step morphodynamics. In turn, the hydraulic jump regime is controlled by several variables as detailed in a new conceptual framework herein. Also in this study, a parsimonious semi-analytical numerical model of step hydraulics is developed to quantify energy dissipation and delineate hydraulic jump regimes, accounting for discharge, jump submergence, and non-uniform channel geometry through a step. Despite remaining limitations in step theory, the model simulates how natural steps respond to a wide range of conditions. The model shows that hydraulic jump regime and energy dissipation exhibit greater sensitivity to channel non-uniformity as discharge increases and/or step height decreases. Also, channel conditions that create greater jump submergence lead to decreased energy dissipation, regardless of the discharge regime. The model also reinforces the common observation about gully erosion that downstream channel widening enhances upstream knickpoint migration. The new algorithm may be used to aid river engineering involving steps and could be useful for landscape evolution modeling.

Keywords: hydraulic jump, energy dissipation, river step, hydraulic geometry, channel evolution
AGU Index Terms: Geomorphology: fluvial (1825), Modeling (1847), River channels (1856)

1. Introduction

1.1 Background

Landscape evolution models are just beginning to account for knickpoint migration in alluvial gullies [*Flores-Cervantes et al*., 2006], but the mechanisms by which lift and drag actually scour the bed below diverse river steps at all landscape positions from bedrock mountain tops to large alluvial rivers remain poorly understood [*Pasternack et al*., 2007]. A key challenge for understanding natural systems arises because experimental studies of hydro-morphologic processes at river steps have previously been simplified with 2-D flume or scale model studies [e.g., *McCarthy and O'Leary*, 1978; *Mason and Arumugam*, 1985; *Lenzi et al*., 2002; *Frankel et al*., 2007]. Natural river steps, however, typically exhibit complex 3-D flow processes [e.g., *Valle and Pasternack*, 2002, 2006a; *Pasternack et al*., *2006*] and occur in non-uniformly shaped channels [e.g., *Sinha et al*., 1998]. A visual confirmation of the natural variability of process and form at river steps is evident in the entries to the world waterfall database (http://www.world-waterfalls.com), which documents 949 waterfalls between ~100-1000 m high and ranging in estimated discharge from ~150-42500 m^3/s. A river step is defined herein as a vertical or near-vertical downstream drop in channel bed elevation, and may be referred to similarly as a waterfall, cascade, knickpoint, headcut, or downstep. This study addresses the fluid mechanics of steps relevant for eventual process-based simulation, regardless of their degree of complexity using a control volume approach in which upstream and downstream conditions constrain internal step processes.

Studies of knickpoint migration in uniform alluvial gullies presently provide the most developed basis for proposed equations for use in landscape evolution modeling, but they only

address the subset of natural steps that have significant plunge pools and they do not include the important role of the lift force exhibited by the flow on the substrate. The form of the shear-stress equation that is typically assumed to govern step migration rate, and thus long-term channel incision in such alluvial gullies, posits that the migration rate increases as discharge increases, because a higher discharge is expected to yield a higher shear stress on the bed below a step [*Alonso et al.,* 2002; *Flores-Cervantes et al*., 2006]. Experimental flume studies do not consistently confirm that expectation, though there is always experimental error to consider. *Slattery and Bryan* [1992] reported a general increase in migration rate with discharge, but *Robinson and Hanson* [1996] reported a lower rate at higher discharge. *Bennett et al*. [2000] found no statistically significant relation among nine experimental runs, though the lowest observed migration rate did occur at the highest discharge. Beyond gullies, researchers have also applied shear stress models to bedrock rivers and determined that channel incision generally occurs locally around steepened knickpoint faces [*e.g., Seidl and Dietrich,* 1992; *Stock and Montgomery,* 1999]. On the basis of geomorphic studies of non-vertical, sloped waterfalls in Japan, *Hayakawa and Matsukura* [2003] proposed that the erosive stress on the face of a falls should be proportional to the square of the discharge.

Two important mechanisms help explain why bed shear stress at the base of a step does not necessarily have to increase as a function of discharge when considering any arbitrary river step. First, steps with a 3-D plan-view brink geometry (e.g. horseshoe falls, oblique falls, and labyrinth weirs) exhibit stage-dependent convergence and/or divergence of flow. *Pasternack et al*. [2006, 2007] showed that at low discharge, flow over a horseshoe falls converges strongly causing higher shear stress. As discharge increases, flow convergence decreases enough to yield a net decrease in local shear stress. *Pasternack et al*. [2007] experimentally observed lower

downthrust stresses for correspondingly higher discharges while holding hydraulic jump regime constant. They also noted that these values could not be accurately predicted using the mathematical approaches suggested in the preceding paragraph to predict erosion in gullies.

Second, shear stress on the bed below a step may decrease even as discharge increases because velocity at the bed is dependent on the hydraulic jump regime, and the latter may change as discharge increases [*Pasternack et al.,* 2006], causing a decrease in shear stress at higher flows. Some previous geomorphic research has discussed the role that hydraulic jumps have in flow mechanics and channel evolution [e.g., *Kieffer*, 1987; *Carling*, 1995; *Grant*, 1997; *Montgomery and Buffington*, 1997]. Hydraulic jumps occur as rapid transitions from supercritical to subcritical flow [*Chanson, 1999*], and are recognized to be controlled by variations in channel geometry and/or stream discharge [e.g., *Mossa et al.*, 2003], but the extent of this control is largely unknown [*Balachandar et al.*, 2000]. In experimental flume studies, it is possible to manipulate the hydraulic jump regime independently of discharge through the use of a sluice gate downstream of the step. By lowering the gate, flow can be reduced, thereby increasing water depth downstream of the step (i.e. "tailwater" depth). In nature the analogous mechanism for tailwater control is the hydraulic geometry associated with channel size and shape as well as discharge. A detailed characterization of hydraulic jump regimes at steps is presented below in section 2.4, and an explanation of the role of hydraulic geometry at a step is presented in section 2.2. As of yet, no studies have systematically explored lift and drag forces below steps over the full range of hydraulic jump regimes. Studies of hydraulic jumps at the toe of dam spillways have shown that jumps are capable of creating hydraulic forces that can weaken and erode such structures [e.g., *Smith*, 1976; *Fiorotto and Rinaldo*, 1992; *Vischer and Hager*, 1998]. Based on experimental measurements, bed-material can be plucked by turbulent pressure fluctuations and

strong lift forces under hydraulic jumps [*Bollaert and Schleiss,* 2003; *Pasternack et al*., 2007]. Plucked material can then be exported by the high drag forces just downstream of jumps [*Bormann and Julien,* 1991; *Pasternack et al*., 2007]. In terms of knickpoint migration in gullies, no experimental studies have systematically manipulated hydraulic jump regime to ascertain its effect on migration rate. It is known that as the plunge pool deepens, the force of the jet impinging at the bottom of the pool decreases. Similarly, it is conjectured that as a hydraulic jump or plunge pool becomes increasingly submerged with increasing discharge, the deceleration of the impinging jet would dampen pressure fluctuations on the bed and lift fluctuations above it. These effects provide another reason why the rate of knickpoint retreat would not necessarily increase with discharge. Hydraulic jump regime is therefore likely to be an important aspect in river step mechanics, but it is largely controlled by channel geometry. Lacking experimental studies to clarify these issues, the opportunity exists for new theoretical developments.

In previous research on river steps, the effect of variability of channel geometry upstream and downstream of a step on step hydraulics has not been investigated. A few studies of engineered spillways have discussed the use of downstream channel widening as an energy dissipater [e.g. *Ram and Prasad*, 1998; *Ohtsu et al*., 1999]. However, studies of man-made dams and spillways address a very narrow range of channel conditions in which a single optimal design is sought. In contrast, natural channels can expand or constrict through a step to any arbitrary degree yielding diverse nappe trajectories (i.e. water profiles over the vertical drop) and hydraulic jump conditions (including the absence of a jump) whose combined effects on energy dissipation, bed scour, and step migration are presently unknown.

Based on the above analysis of past studies, a key limiting factor in understanding and predicting scour at river steps is associated with understanding the stage-dependence of river-step

fluid mechanics. The focus of this study was to use a numerical model to heuristically investigate channel hydraulic geometry and discharge in determining the hydraulic jump regime and energy dissipation at a river step. Specific objectives included predicting the hydraulic jump regime and energy dissipation as (1) discharge varies for a given channel geometry, (2) channel geometry varies for a given discharge, and (3) channel geometry upstream of a step varies relative to that downstream of it. The approach involved a purely theoretical framework in which available analytical and empirical equations were coupled to yield a new parsimonious model formulation. Admittedly, the resulting numerical model has several assumptions and limitations, but it does provide a strong heuristic explanation of why erosion at river steps is not a direct function of only discharge. It also elucidates the key scientific gaps that need to be addressed to promote further advancement.

Although the study presents detailed fluid mechanics results, the general conclusions are relevant to a variety of applied water resources problems involving natural and man-made river steps. One value of this work is that it provides a new and different approach to predicting erosion at river steps in channels with variable geometry in landscape evolution models. This model does not yet predict scour directly yet, but it predicts hydraulic jump regime and energy dissipation, which are both important factors controlling bed scour below steps. Another value is that river rehabilitation and engineering project conceptual models, including those for dam removal, fish passage, and whitewater parks, often employ steps, but do not consider the importance of channel geometry in controlling the safety and functionality of these hydraulic structures. This model provides a tool that would be of immediate value in improving the safety of hydraulic structures.

1.2 Step Conceptual Framework

The role of hydraulic jump regime in scour at the bottom of a river step is not widely understood. Very few experimental studies of river steps have varied the hydraulic jump regime over the full range possible to explore this factor. To promote a better understanding of the general relevance of hydraulic jumps associated with river steps for water resources management and to guide research ultimately leading to prediction of river step morphodynamics, a conceptual model encompassing independent variables and responding processes was developed in which the key dynamics were grouped into five categories (Figure 1). Evolution of a river step can be characterized by the processes of scour hole formation, upstream retreat, and change in step geometry. These processes are driven by a complex, interdependent set of hydrologic and geologic variables acting over multiple scales. Basin variables include the independent watershed inputs of water and sediment discharges as well as channel geology (Figure 1). For example, some steps may exist in various geologic conditions ranging from well-bedded sedimentary bedrock to fractured homogeneous igneous bedrock. The role of sediment supply has been an important recent addition to shear stress models [*e.g. Sklar and Dietrich*, 2004; *Gasparini et al.,* 2007]. The basin variables control the channel variables, which include the cross-sectional geometries within the channel, the channel slope, and the longitudinal spacing between river steps. In this framework, a sequence of cross-sections is used as an indicator of complex 3-D channel morphology, since channel width and cross-sectional area often fluctuate down a mountain river system, even as they generally increase downstream due to increasing discharge. Basin variables also help shape the step morphology components of step height, planform shape of the step, step slope, and step roughness. Step height can be dependent upon step spacing [*Wohl and Grodek*, 1994].

All of the step morphology variables affect step hydraulics characterized by the nappe trajectory and hydraulic jump regime, though step roughness only affects the jump regime indirectly through nappe trajectory. Nappe trajectory and hydraulic jump regime are of central importance in the conceptual model, because a) the former is a key variable controlling jet scour of bedrock near the step toe [*Mason and Arumugam*, 1985; *Bormman and Julien*, 1991; *Stein et al.,* 1993; *Alonso et al*., 2002], where toe refers to the slope break at the bottom of the step, and b) the latter controls turbulent lift forces that pluck and suspend bedrock downstream of the point of jet impact [*Fiorotto and Rinaldo*, 1992; *Pasternack et al*., 2007]. Nappe trajectories for linear overfalls have been thoroughly investigated [*USBR, 1948b*; *Vischer and Hager;* 1998*; Chanson,* 2002], while those for overfalls with 3-D brink configurations have only recently come under some scrutiny [*Falvey*, 2003; *Pasternack et al*., 2006]. Hydraulic jump regimes for a free overfall include: supercritical flow with no jump, pushed-off unsubmerged jump (defined later in Section 2.4), optimal jump, submerged jump, standing waves, and subcritical flow with no jump [*USBR, 1948b; Leutheusser and Birk,* 1991]. Hydraulic jump regime is strongly influenced by discharge and tailwater depth [*USBR, 1948b*; *Pasternack et al*., 2006], with the latter in turn controlled by upstream and downstream channel configuration. Step brink planform shapes that deviate from linearity cause nappe interference and a shift in jump regime for a given discharge and channel configuration [*Falvey*, 2003; *Pasternack et al*., 2006]. Additionally, the nappe regime has been anecdotally observed to be affected by the direction and magnitude of wind impacting it, but no scientific studies have yet explored nappe response to diverse wind regimes.

Step hydraulics such as jet impact, turbulent pressure fluctuations, drag, and lift drive channel morphodynamics by changing the size and shape of the scour hole [*Lenzi et al*., 2003; *Alonzo et al*., 2002], step geometry [*Pasternack et al*., 2006], and upstream retreat of the step

[*Hanson et al*., 1997; *Bennett et al*., 2000; *Stein and LaTray*, 2002]. Upstream retreat is determined by the relative erodibility and erosional force on the step top versus that on the face and toe of the step [*e.g., Stein and Julien*, 1993; *Flores-Cervantes et al*., 2006; *Frankel et al*., 2007]. The shape of the scour hole and the regime of the associated hydraulic jump affect the erosional ability of the flow below the step. Scour depth has previously been shown to be dependent on step morphology [*Alexandrowicz*, 1994; *Lenzi et al*., 2002] and sediment supply [*e.g., Marion et al*., 2006]. Step morphodynamics, in turn, can affect channel geometry and step morphology.

The conceptual framework described above serves to organize past research, promote quantification of identified linkages, and highlight important gaps in the current understanding. A casual observer of major waterfalls and whitewater rapids in mountain rivers will quickly take note of the diversity and complexity of natural step morphologies. Addressing natural diversity presents the most important gap in the scientific understanding of river steps. This study addresses the problem of how channel expansions and constrictions through geomorphic units with steps affect step fluid mechanics.

2. Step Systematics

Although it is impossible at this time to produce a numerical model that incorporates all of the processes discussed in section 1.2, that conceptual framework can serve as a roadmap to guide process-based research leading toward an eventual predictive capability. The first phase of developing a suitable numerical model requires starting at the step itself and adequately characterizing step hydraulics on the basis of step morphology and surrounding channel variables.

The quantitative formulation used below is very different from that proposed previously for gullies [*e.g. Alonso et al.,* 2002; *Flores-Cervantes et al.*, 2006]. Admittedly, this approach has limitations and uncertainties, but the results in Section 3 provide new insights that shed light on how river steps likely evolve over time as a result of natural spatial variation in channel geometry.

2.1 Eulerian Governing Equations

As an introduction to the broader 3-D problem, consider steady energy and momentum conservation for a control volume in a level rectangular channel with clear water including a broad-crested bed overfall and the region downstream of the step (Figure 2). There holds for average conditions the following classic hydraulic equations [e.g., *USBR, 1948b; Ackers et al., 1978; Chaudry, 1993; Chanson, 1999; Munson et al., 2006*]:

the overall energy conservation equation:

$$E_{up} = (H + P) = (h_d + h_{tail}) = E_{tail} + h_L \quad (1)$$

a rearrangement of equation (1) that solves for the submergence variable, h_d:

$$h_d = h_L + h_{v\_tail} = h_L + \frac{q^2}{2gh_{tail}^2} \quad (2)$$

the mass conservation equation that is valid for any cross-section, *i*:

$$q = v_i h_i \quad (3)$$

a special case of equation (1) that solves for the critical flow condition:

$$h_c = \left(\frac{q^2}{g}\right)^{1/3} \quad (4)$$

the definition of Froude Number at location *i*:

$$Fr_i = \sqrt{\frac{q^2}{gh^3}} \quad (5)$$

and the broad-crested weir equation derived from equations (1) and (4):

$$q = (2/3)^{3/2} C_b \sqrt{g} H^{3/2} \quad (6)$$

where E_i and h_i are total energy and water depth at any location i as defined in Figure 2, H the specific energy at the upstream location (weir crest as datum), P the broad-crested step height, q the specific discharge, h_L the total energy loss in the control volume, g the gravitational constant, v_i the velocity at location i, and C_b=0.848 the broad-crested weir discharge coefficient [*Ackers et al.*, 1978; *Leutheusser and Birk*, 1991; *Chanson*, 1999]. For the equations presented above and throughout this text, the subscript "up" refers to the channel section upstream of the step, and the subscript "tail" refers to the controlling channel section downstream of the step and associated hydraulic jump regime (Figure 2). Equations (4)-(6) assume a rectangular channel, and are approximate for a wide channel of any shape. They are not, however, ultimately used in the new numerical model presented herein, thereby representing a significant advance and eliminating that concern.

In past studies momentum conservation was used to isolate the head loss solely due to the hydraulic jump for the classic hydraulic jump [*Chanson*, 1999] and unsubmerged jumps at overfalls [*Henderson*, 1966]. In those cases there exists an identifiable upstream supercritical cross-section and downstream subcritical cross-section bounding the jump. The Belanger Equation has also been modified to describe the unsubmerged hydraulic jump for non-prismatic channels [*Negm,* 2000]. However, these approaches are invalid when the hydraulic jump is submerged because the equation necessitates a measurable upstream supercritical depth value, but the supercritical jet is underwater. As the model developed herein encompasses all hydraulic jump regimes, including submerged jumps, the classic Belanger Equation is not used and it is thus not possible to isolate the energy dissipation of just the jump.

Critical depth is often used to non-dimensionalize variables; however, locating the critical point introduces error [*Ackers et al*., 1978], whereas defining upstream specific and total energy is more practical and certain. In addition, the variable *(H+P)/H* is the non-dimensional energy variable accounting for both discharge and step height [*USBR, 1948b*]. It shows that geometric scaling to yield any energy condition is achievable by holding either step height or flow constant. Higher *(H+P)/H* values correspond with taller steps with relatively less flow over them. As discharge increases for a given step height, so does the head on the step. Therefore decreasing *(H+P)/H* values represent conditions of increasing discharge and increasing energy input for a given step height. In the lower limit of no step (P=0), the variable approaches unity.

In this study, "submergence" is defined as the condition when h_{tail} is deep enough to place the leading edge of the jump upstream of the location of the free-falling nappe toe [*Leutheusser and Birk,* 1991], where the nappe toe is defined as the slope break in the water surface profile downstream of the step. According to classic equations (1)-(6), when *(H+P)/H* and the non-dimensional submergence variable (h_d/H) are specified, the resulting $h_L/(H+P)$ and flow kinematics at upstream and tail cross-sections are independent of step geometry [*USBR, 1948b*; *Pasternack et al*., 2006]. However, the degree of submergence and hydraulic jump regime are dependent on aspects of step geometry, notably planform brink shape and step slope.

Whereas engineers classically solved equations (1)-(6) to find optimal spillway and overfall designs for engineered structures to minimize damage to such structures [e.g. *Moore*, 1943; *White*, 1943; *Henderson*, 1966], those studies did not tackle the broader water resources problem facing natural channels in which step fluid mechanics responds to a very wide range of non-optimal upstream energy and downstream submergence conditions. For example, there exist many steps in bedrock rivers that exhibit supercritical jets impinging on exposed bedrock and

continuing on as supercritical flow; peruse the world waterfall database at http://www.world-waterfalls.com to see many examples of this phenomenon. There are also many steps with submerged jumps due to the presence of a plunge-pool. While transference of classic engineering foundations to the problem of understanding natural 3D waterfalls has value, the unique aspects of natural systems warrant further investigation. *Pasternack et al*. [2006] addressed this broader problem by solving equations (1)-(6) for fractional energy dissipation $h_L/(H+P)$ for a larger non-classical range of submergence h_d/H and energy $(H+P)/H$. Unlike in laboratory flumes with sluiced inflows, the upstream *Fr* approaching a step in a natural channel is not an independent variable, so it is not a governing variable for natural systems. The results showed that the maximum $h_L/(H+P)$ for any $(H+P)/H$ occurs when h_{tail} is exactly critical with no hydraulic jump present. This maximum involves a transition from supercritical to critical flow and $h_{toe}<h_{tail}$. Also, as h_{tail} is decreased to less than critical depth, $h_L/(H+P)$ decreases and the flow increases its efficiency until $h_{toe}=h_{tail}$. The primary conclusion from their analysis was that arbitrary h_{tail} must be included in models of flow kinematics and energy dissipation at natural river steps.

2.2 Channel Parameterization

Even though *Pasternack et al*. [2006] used the classic equations (1)-(6) to expand the breadth of the relevance of those equations into non-classical water resources problems, their model assumed a uniform rectangular channel, because that was their flume set-up for experiments on a broad-crested horseshoe waterfall. In this study, equations (4)-(6) were replaced to further generalize the model to reduce or eliminate the assumptions of a rectangular channel, a 2-D overfall, and mutual independence of $(H+P)/H$ and h_d/H. Arbitrary upstream and downstream cross-sectional morphologies are now enabled and characterized using another

classic principle from a different branch of river science, namely empirical at-a-station hydraulic geometry relations originally stemming from channel regime theory [*Garde and Ranga Ragu*, 1985]. Even though such equations are empirically-derived geometric descriptors, they do satisfy mass conservation requirements [*Leopold and Maddock*, 1953] and are widely used by fluvial geomorphologists, who accept them as classic in their discipline. These equations do not assume a rectangular channel. They are used herein to replace equations (4)-(6) to obtain discharge from upstream channel conditions and add more equations to govern channel changes through the geomorphic unit containing the step. As will be shown, they also are used to directly link $(H+P)/H$ and h_d/H, so those two variables are not independent. Although brink geometry and nappe trajectory play an important role in step dynamics, they are not necessary in quantifying the net energy loss between the upstream and downstream cross-sections. Admittedly, both factors affect the jump regime [*Falvey*, 2003; *Pasternack et al.*, 2006] and that remains an important limitation of the numerical model discussed further below. However, the model will clearly illustrate the importance of variable cross-sectional geometry on hydraulic jump regime and energy loss at river steps.

According to classic channel regime theory, at a given cross-section the flow width, depth, and velocity can be related to the volumetric discharge (Q) by the power functions [*Leopold and Maddock*, 1953]:

$$w = aQ^b,\ h = cQ^f, \text{ and } v = kQ^m \qquad (7a,b,c)$$

where w is average channel width, h is average channel depth, v is average flow velocity, $\{a,c,k\}$ are empirical coefficients, and $\{b,f,m\}$ are empirical exponents that largely control cross-sectional shape . Equation (3) governs that $b+f+m=1$ and $a \times c \times k=1$ [*Leopold and Maddock*, 1953]. In this study, b, f, m, a, c, and k are all termed "parameters" of the overall model. No general values for

these parameters have been published yet for bedrock rivers with steps, though such studies appear pending. Several specific values have been published for alluvial rivers [*Wilcock*, 1971; *Drury*, 1976; *Betson*, 1979; *Andrews*, 1984; *Rhoads*, 1991; *Singh*, 2003; *Stewardson*, 2005], with many states in the United States now developing extensive databases stratified by physiographic province. After a review, the published values of the b exponent were found to vary from 0.04 to 0.6, and those for the f exponent from 0.20 to 0.65. Similarly, those of the a coefficient ranged from 3 to 19, with a mean value of 9.74, and those of the c coefficient from 0.474 to 0.73, with a mean value of 0.51. In this study, hydraulic geometry relations are used to describe channel size and shape at one cross-section located upstream of a step and one downstream of it. When applying the numerical model developed in this study to a given real step, one can use monitoring data to parameterize the coefficients and exponents for the cross-sections at that site.

To interpret the results of this study, it is critical to understand the geometric patterns implied by combinations of exponents and coefficients. *Dingman* [2007] provides a detailed mathematical analysis of how to interpret these parameters, and the key concepts are summarized below. Channel shape changes predictably as a function of the exponents, assuming constant coefficients (Figure 3). When $b=f$, the channel is triangular in cross-section. In the limit, as b approaches 0, width does not change as discharge increases. Geometrically, that necessitates that the channel is rectangular when $b=0$. For values of $b<f$, the channel is concave up. Similarly, as f approaches 0, depth does not change as discharge increases. Geometrically, that necessitates that the channel is infinitely wide when $f=0$. For values of $b>f$ (Figure 3, shaded region), the channel is convex up. In summary, when $b \neq f$ and one of those exponents is allowed to change, then the geometric effect is one of "bending" – for increasing f bending is inward and for increasing b, bending is outward. As both b and f approach 0 together, the velocity exponent, m, increases.

Geometrically, a condition of no change to depth or width as discharge increases requires an increase in energy slope and/or a decrease in channel roughness with increasing discharge. It is widely held that roughness decreases as discharge increases [*Smart*, 1999; *Dingman*, 2007]. Similarly, for a meandering channel, valley slope is higher than channel slope at the reach scale, so the energy slope is higher for out-of-bank flows than in-channel flows.

For any given set of exponent values and corresponding channel shape, the values of the coefficients affect the scaling of the channel. A higher value of the coefficient a stretches the banks horizontally (i.e. for a triangular channel, the angle between the banks increases), which makes the wetted channel flatter. A higher value of the coefficient c stretches the banks vertically, which makes the channel higher. Finally, a higher value of the coefficient k is associated with a steeper bed slope and/or a smoother bed at any given discharge.

Although the exact geometries associated with changes in exponents versus coefficients are different (i.e. bending versus stretching, respectively), the effects of both types of changes on the simpler variables of cross-sectionally averaged channel depth and width are similar. For example, increasing either a or b alone in equation (7a) causes the width at any given discharge greater than one to increase (Figure 4). Either change also causes the slope of the tangent line of the relation to increase. Thus in terms of width and depth, changes to both types of parameters yield similar outcomes, even though they do so in different ways geometrically.

Finally, while hydraulic geometry relations can characterize braided or multi-threaded channels, which sometimes are associated with river steps, as exemplified by Great Falls on the Potomac River between Maryland and Virginia (38°59'51 N, 77°15'10 W), the parameters for multi-threaded channels are non-unique and thus difficult to interpret. Although hydraulic geometry equations are empirically derived, they are well suited for parsimonious exploration of

channel non-uniformity at river steps. They are also easily quantifiable at real river steps by mapping the cross-sections upstream and downstream of the step when flow is low and then using automated stage recorders at those locations to record the local stage-discharge responses. Accurate physics-based 3-D hydrodynamics models of the multiphase flow through hydraulic jumps at natural river steps have yet to be achieved, limiting strict physics-based alternatives.

2.3 Channel Non-uniformity

For the independent variables of step height and upstream depth along with the upstream values of the geometric exponents (b_{up} and f_{up}) and coefficients (a_{up} and c_{up}) of equations (7a,b), the resulting relative submergence and head loss through the step (equations. 1 and 2) are determined from the following set of equations. For the equations presented here, the subscript "up" refers to the channel section upstream of the step, and the subscript "tail" refers to the controlling channel section downstream of the step and hydraulic jump regime (Figure 2).

Rearranging equation (7b), discharge is determined at the upstream cross-section as:

$$Q = \left(\frac{h_H}{c_{up}} \right)^{\frac{1}{f_{up}}} \tag{8}$$

where h_H is the effective flow depth above the step crest. Again, this equation does not assume a rectangular channel. As shown in Figure 2, h_H can be determined by:

$$h_{II} = h_{up} - P \tag{9}$$

For varying effective step heights for the upstream and downstream channel sections, the definition of h_H remains the same, but the calculation of depth may differ. This definition accounts for the physical reality that the water from h_{up}=0 to h_{up}=P is "dead" storage that does not affect the dynamics of the step, i.e. there can be no tailwater until this volume is filled. Figure 2

represents the geometry of this dead storage with an arbitrary channel bottom, which means there could be a step up for the flow or the channel bottom could be flat and planar leading up to the step drop. In either instance, that geometry does not affect the equations used in this model. In practical application, one would develop an upstream hydraulic geometry relation referenced to the step crest elevation instead of the channel bottom as most are.

Next, the tail depth is determined for the controlling downstream cross-section at the exit of the tail pool as:

$$h_{tail} = c_{tail} Q^{f_{tail}} = c_{tail} \left(\frac{h_H}{c_{up}} \right)^{\frac{f_{tail}}{f_{up}}} = c_{tail} \left(\frac{h_H}{c_{up}} \right)^{\frac{1}{fratio}} \quad (10)$$

where *fratio* is the ratio of the upstream *f* exponent (f_{up}) to the downstream *f* exponent (f_{tail}). An *fratio* of one describes a uniform channel consistent with the previous assumption of *Pasternack, et al*. [2006]. An *fratio*<1.0 refers to a system in which flow transitions from a wider, more triangular channel into a narrower, taller canyon such that the upstream depth rises slower than the downstream depth as discharge increases (Figure 5). Examples of this are ubiquitous in mountain channels (e.g. Figure 6). A similar effect on width and depth could be achieved by having a lower *c*-value upstream and a higher *c*-value downstream, though the exact geometric interpretation would be different, since the non-uniformity would be due to stretching, as described earlier. Also, c_{up} is scaled by the *fratio* in equation (10), and this indirect effect on h_{tail} is synergistic with the direct effect of the *fratio*, though the relative magnitude of the effect will be evaluated in the results later. For example, if c_{up}=0.51 and *fratio*=0.50, then $c_{up}^{1/fratio} = 0.26$. This smaller value in the denominator makes h_{tail} bigger for any given discharge, and thus is consistent with a deeper constricted channel downstream. An *fratio*>1.0 refers to the opposite effect as just described. In this case, flow transitions from a narrower, more triangular channel

into a wider, flatter channel (Figure 7). Many natural example of this type of transition can be found in mountain rivers, as well (e.g. Figure 8). If c_{up}=0.51 and *fratio*=1.5, then $c_{up}^{1/fratio} = 0.64$, so the coefficient effect is smaller than for an equivalent incremental change of *fratio* when *fratio* <1. In both cases, the step is located in the transitional region, and is thus impacted by the non-uniformity. To fully understand the consequences of using at-a-station hydraulic geometry relations to characterize channel non-uniformity, sensitivity analyses were performed over a wide range of model parameters, as discussed further below in Section 2.5.

Upstream and downstream widths are determined from hydraulic geometry relations based on the discharge obtained in equation (8):

$$w_{up} = a_{up}Q^{b_{up}} \text{ and } w_{tail} = a_{tail}Q^{b_{tail}} \quad (11a,b)$$

Insufficient literature exists on the interactions of *b*, *f*, and *m* values for at-a-station conditions in the vicinity of river steps to precisely constrain *b*-values at this time. However, it is conceptually evident that as a channel's *f*-value increases a channel becomes more rectangular and thus the *b*-value must decrease (Figure 3). *Dingman* [2007] quantitatively demonstrated this for three different hydraulic equations. On this basis, the ratio of upstream and downstream *b* values was assumed to be equal to the inverse of the *fratio*. Future field investigation may enable revision of this assumption, but it is expected to only affect magnitudes of effect and not cause threshold effects.

The cross-sectionally averaged upstream and downstream velocities and corresponding averaged velocity heads were determined from equation (7c) and calculated as:

$$v_{up} = k_{up}Q^{m_{up}} \quad v_{tail} = k_{tail}Q^{m_{tail}} \quad \text{and} \quad h_{v\_up} = \frac{v_{up}^2}{2g} \quad h_{v\_tail} = \frac{v_{tail}^2}{2g} \quad (12), (13)$$

where the coefficients, k, and exponents, m, are solved from mass conservation (k=1/ac and m=1-(b+f) [*Leopold and Maddock,* 1953]. These equations do not assume a rectangular channel.

The upstream specific energy (H) is the effective head on the step (Figure 2), and is calculated as:

$$H = h_H + h_{v\_up} \quad (14)$$

Thus the key variables of submergence, h_d, (equation 2) and head loss, h_L, (equation 1) can now be non-dimensionalized as h_d/H, and $h_L/(H+P)$ in conjunction with the other key variable, non-dimensional upstream energy, $(H+P)/H$, to define the Eulerian fluid mechanics of a river step.

2.4 Hydraulic Jump Regime Equations

Previous researchers have developed threshold equations for hydraulic jump regimes. Most such equations delineate jump regimes using only the Froude number on the basis of observations of the classic hydraulic jump in a rectangular flume with no bed step, where variable *Fr* is imposed using an upstream sluice gate [e.g. *Chanson*, 1999]. For the non-classical case of non-uniform channels with overfalls, jump regime equations must account for jump submergence. Of the published equations, only those of *USBR [1948b]* for an ogee-crested 2-D overfall and those of *Pasternack et al*. [2006] for a broad-crested, rectangular overfall do that (Figure 9). The thresholds of *USBR* [1948b] are empirically derived and, most importantly, non-dimensional. Those of *Pasternack et al*. [2006] are semi-analytical and only address two regimes- the critical *Fr* and optimal jump thresholds. Conceptually similar regimes for a sharp-crest weir were described by *Leutheusser and Birk* [1991], but not quantified. It is possible to modify and use the model of Pasternack et al., [2006] to establish the critical *Fr* threshold for a sharp-crested weir.

More investigations into regime equations for typical 3-D overfall brink configurations are needed.

Accepting the limited availability of relevant equations, Figure 9 shows the four empirical regime boundaries used in this study that were first described by *USBR* [1948b] for an ogee-crested weir. The top curve represents the threshold above which flow over the step remains supercritical and cascades past the tail cross-section. The threshold curve below that delineates the optimal jump condition with the jump occurring exactly at the step toe. The condition that lies between those thresholds represents emerged, or pushed-off, hydraulic jumps with a measurable supercritical zone and rapid transition to a subcritical zone within the control volume. The next curve below delineates jumps that are sufficiently submerged to be considered "drowned", which is undefined by *USBR [1948b]*. Drowned jumps are interpreted to mean those submerged jumps with a strong upstream recirculation. The bottom line in Figure 9 represents the threshold below which no hydraulic jump occurs, with the flow having either standing waves or no near-critical surface expression at all. There is no regime uniquely delineated for a standing wave condition in the *USBR [1948b]* framework, which is a detriment. Overall, this quantitative framework serves to delineate well-recognized jump types, each with characteristic fluid mechanics in terms of jet impact force, turbulent pressure fluctuations, drag along the bed, and lift force.

The threshold equations of the ascribed conditions for $2 \leq (H+P)/H \leq 6$ (Figure 9), with the corresponding terminology of *Leutheusser and Birk* [1991] given in parentheses, are:

Pushed-off Jump (Swept-out Jump)
$$\frac{h_d}{H} = 0.998\left(\frac{H+P}{H}\right) - 0.595 \quad (15)$$

Hydraulic Jump (Optimum Jump)
$$\frac{h_d}{H} = 0.918\left(\frac{H+P}{H}\right) - 0.913 \quad (16)$$

Drowned Jump (Plunging Nappe) $$\frac{h_d}{H} = 0.176\left(\frac{H+P}{H}\right)^{1.679} \quad (17)$$

No Jump (Surface Nappe) $$\frac{h_d}{H} = 0.16 \quad (18)$$

The above equations provide a reasonable characterization of the hydraulic jump regimes at or downstream of a step toe. Substituting the equations of *Pasternack et al*. [2006] for Equations (15, 16) produce a very small change in the lines, with minimal conceptual difference.

One important limitation of these equations is that they do not account for the effects of non-uniform step brink geometry on jump regime (i.e. whether in plan view the brink is horseshoe shaped, perpendicular to the banks, oblique to the banks, etc). *Pasternack et al*. [2006] describe the deviations from these conditions associated with horseshoe-shaped brinks, such as that of Niagara Falls. Another limitation of the equations is that they do not account for regime deviations associated with abrupt channel expansions or constrictions. Additional factors that could affect the equations include step and plunge-pool roughness, plunge-pool depth, bedrock resistance, and high winds. Because the jump regime is influenced by so many variables, it is not apparent how to further generalize these equations other than by careful study of each possible archetypal configuration. Nevertheless, this study provides a first assessment as to how the most important forms of channel non-uniformity would affect hydraulic jump regimes.

2.5 Model Implementation

Equations (1), (2), and (8) – (14) were programmed into Excel 2003 [*Microsoft Corp, Redmond, WA*] to investigate the effect of varying upstream and downstream channel geometry, in conjunction with discharge and step height, on flow processes, hydraulic jump regime, and energy dissipation associated with a river step. The key independent variables were *(H+P)/H* and

fratio, with f_{up}, b_{up}, a_{up}, and c_{up} serving as key parameters. The non-dimensional response variables evaluated were h_d/H, indicative of hydraulic jump regime, $h_L/(H+P)$, a measure of energy loss, and $h_{v\_tail}/(H+P)$, a measure of kinetic energy.

The computational procedure for the model begins with a set of starting values {a_{up}, c_{up}, b_{up}, f_{up}, *fratio,* h_H, and P}. From the upstream depth and hydraulic geometry values, a discharge is calculated (equation 8) for that depth. The upstream width and specific energy (H) are calculated using equations (11a) and (14). Using the given *fratio*, the downstream hydraulic geometry parameters are calculated, and then the model calculates the downstream depth, width, and specific energy (Eqs 10 – 14). Equations (1) and (2) are then used to determine the head loss, h_L, and submergence, h_d. These variables and the total energy ($H+P$) are non-dimensionalized by the upstream specific energy, H.

Plots of these response variables as a function of $(H+P)/H$ were made for nine combinations of upstream *f* and *b* values from the set {0.2, 0.25, 0.4} to explore the sensitivity of the model to the absolute value of each parameter. Values of *f* or *b* higher than 0.4 did not yield substantially different results than those shown for 0.4, and hence are not presented here. For each combination of *b* and *f*, six values of *fratio* {0.5, 0.75, 0.9, 1.0, 1.25, 1.5} were used in the model to investigate its influence on river step response. For these ranges of *f* and *b* values that were used, the model yielded ranges of discharge from 3 – 104,000, upstream width from 12 – 400, and upstream depth from 0.8 – 5.5 among the six combinations of *fratios*. These variables have typical dimensions, but specific units are purposefully omitted to allow the model to be applied to any channel system within any system of units. These analyses therefore capture the essential functionalities and sensitivities of the model with respect to the exponents, and through them natural steps.

To explore the effects of the coefficients of equations (7a, b, c), a sensitivity analysis was performed in which the range of reported values for a and c were investigated. The analysis consisted of holding the upstream b and f values constant, while varying the geometric coefficients, a and c, for the range of modeled *fratios*. In these tests, $a_{up}=a_{tail}$ and $c_{up}=c_{tail}$. Two combinations of f_{up} and b_{up} were evaluated, namely $f_{up}=b_{up}=0.2$ and $f_{up}=b_{up}=0.4$. Future versions of the model could solve for the model parameters based on various theories that attempt to explain their origin, but in this study the goal was to provide a characterization of the effects of their values on river step hydraulics.

Currently, this model is purely theoretical. As with many models in hydrology and geomorphology, including distributed hydrological models, 3D hydrodynamic models, and landscape evolution models, this one is out in front of the experimental capability to validate all of its components. No datasets presently exist to test the range of the model. To empirically satisfy the physicality of the model would require laboratory equipment that varies upstream and downstream channel geometries through a suite of combinations, or locating natural study sites that fit the suite of combinations. It would then be necessary to carefully measure the hydraulic terms and estimate energy dissipation, which is something that *Henderson* [1966] describes as extremely challenging to do accurately. The model consists of a manipulation of classic hydraulic and geomorphic equations, and thus should be technically sound. It provides first insights into energy dissipation and hydraulic jump regimes for non-uniform channels and a roadmap of key variables deserving of further experimental investigation. An attempt has been made to fully express all assumptions and limitations upfront.

3. Results

To understand the effects of channel non-uniformity on hydraulic jump regime and energy dissipation at river steps, it is first important to understand how width and depth vary through the section in response to changes in discharge and *fratio* (Figure 10). As b_{up} increases for a given *fratio* and constant f_{up}, the downstream width-to-depth ratio also increases (*e.g.* Figure 10g, h, i). As f_{up} increases for a given *fratio* and constant b_{up}, the downstream width-to-depth ratio decreases (*e.g.* Figure 10i, f, c). In general, however, the geometric width exponent, b_{up}, has a greater affect on the downstream width-to-depth ratio than f_{up} (Figure 10).

For the cases of $f=b$ and an *fratio*=1.0, the model shows the expected results of the downstream width-to-depth ratio remaining constant for the range of discharge evaluated (Figures 10c, e, g, diamonds), while increasing the *fratio* increases the downstream width-to-depth ratio (*e.g.* Figure 10c,e, g, circles). Decreasing the *fratio*, however, decreases the downstream width-to-depth ratio (*e.g.* Figure 10c, e, g, triangles). The responses to either case of varying *fratio* become more dramatic as discharge increases.

These patterns as a function of *fratio* comprehensively confirm the interpretations illustrated in Figures 5 and 7 over the full range of exponent values explored. When $f_{up}=b_{up}= 0.4$ and *fratio*=0.5, the geometric interpretation is that the channel is bending and stretching to a more concave up cross-section through the step (Figure 5). The hydraulic shape of the downstream channel shows that depth will increase much faster than width as discharge increases (Figure 10c, circles). For the same upstream model parameters, but an *fratio*=1.5, the geometric interpretation is that the channel is bending and stretching to a more convex up cross-section through the step (Figure 7). The downstream channel shape will create a greater response to flow width than flow depth as discharge increases (Figure 10c, triangles). As an example, the specific values of widths and depths for two flow stages shown in Figures 5 and 7 quantify the differences in the rates of

change. For the low *fratio* example, the ratio of the upstream widths between the two discharges is about five, and this ratio decreases through the step to 2.2 at the downstream cross-section (Figure 5). For the high *fratio* example however, those width ratios increase from five to 11 (Figure 7). In summary, the results demonstrate that manipulation of the *fratio* in the model effectively simulates non-uniform channel constriction and expansion through a river step. In the following subsections, the fundamental response of a river step to different flow magnitudes and different ways of manipulating channel non-uniformity is explored with respect to downstream hydraulic jump regime and energy loss at the step.

3.1 Role of Energy Input

This model re-captures the basic response of the river step to increasing discharge for a uniform channel with relatively high values of f and b as previously demonstrated by *Pasternack et al*. [2006]. Consider the case of the uniform channel (*fratio*=1.0) with f and b values of 0.4 each (Figure 11c, diamonds). For high $(H+P)/H$, the step is relatively high and thus there exists a drop over the step yielding a hydraulic jump at the step toe. Model results show that the highest fractional energy loss occurs at the lowest energy input regardless of geometric combination, because a high fall yields a conversion of potential energy into kinetic energy, and this large amount of converted energy cannot be recovered as potential energy through the hydraulic jump at the base of a high drop (*e.g.*, Figure 12c). When the flow has reach the downstream cross-section, the kinetic energy is greatly dissipated, representing <0.1% of the total energy (*e.g.*, Figure 13c). As $(H+P)/H$ decreases, the tail depth increases and the water drop height decreases, causing the jump to submerge. In the limit as $(H+P)/H \rightarrow 1$, the hydraulic jump gives way to a standing wave and ultimately no surface expression at all. Correspondingly, there is less potential

energy to be dissipated as the jump submerges, so the submerged hydraulic jump helps reduce the energy loss at the step (Figure 12c). Also, since the kinetic energy increases at the upstream cross-section with increasing energy input, it also shows the same functionality at the downstream cross-section (Figure 13c). In the limit as $h_d/H \rightarrow 0$, simple hydraulic geometry relations no longer apply, as the step is fully submerged and the downstream depth becomes the control for the upstream depth. The overall mechanics reported above represent the classic 2-D step behavior for a uniform channel. However natural mountain rivers have strongly non-uniform channels and 3-D planform brink geometries, thereby creating a wide array of conditions remaining to be understood.

3.2 Channel Non-uniformity

To fully understand the dependence of the downstream geometry on the upstream parameters and the *fratio* used in this model, consider a channel with the upstream channel geometry is defined by the hydraulic exponents (f_{up} and b_{up}) are equal to 0.2 (Table 1g). For an *fratio* of 1.5, the *bratio* is equal to the inverse, i.e. 1/1.5 = 0.67. The definition of *fratio* is the ratio of f_{up} to f_{tail}, therefore the value for the downstream *f* value decreases to 0.13. Since the *bratio* is the inverse of the *fratio*, the downstream *b* value increases from 0.2 to 0.3. Table 1 presents the range of hydraulic exponents explicitly used in this model.

Consider again the case of the upstream channel geometry having f_{up} and b_{up} values of 0.4 each (Figure 11c). Using the results associated with an *fratio* of 1.0 described above as the baseline, the model shows the effect of varying the downstream geometry on the hydraulic jump regime for a given discharge and step height. As the *fratio* for the channel increases above one, the downstream cross-section bends and stretches outward, so water depth decreases, width

increases, and the hydraulic jump becomes increasingly emergent. For an *fratio* of 1.5, the zone of the supercritical flow regime increases until $(H+P)/H<3$ and there is no hydraulic jump present within the downstream control volume. In contrast, as the *fratio* for the channel decreases below one, the downstream cross-section bends and compresses inward, so water depth increases, width decreases, and the hydraulic jump increasingly submerges for constant $(H+P)/H$ to a point where no jump or standing wave feature is present. For example, when *fratio*=0.5, there is no surface expression of the step for $(H+P)/H<3.76$. As both f_{up} and b_{up} decrease together, the upstream velocity exponent, m, must increase. The associated acceleration of flow decreases depth and width at any given discharge, and thus the model shows that as m increases, the hydraulic jump regime becomes more emergent for all *fratios* (Figure 11c, e, g). For example, when a channel with $f_{up}=b_{up}=0.4$ is compared to one with $f_{up}=b_{up}=0.25$ at an *fratio*=0.75 (Figure 11c, e, crosses), the former shows a wide range of hydraulic jump regimes for $2<(H+P)/H<6$, while the latter only exhibits the pushed-off and optimum-jump regimes.

A non-uniform channel with an *fratio*>1 exhibits more relative head loss than one with *fratio*<1 for all geometric combinations (Figure 12). The dominant cause of head loss at river steps is the difference in potential energy at the upstream and downstream cross-sections, since kinetic energy is extremely difficult to recover as potential energy and tends to dissipate through multiple scales of turbulence and bed interaction. For high values of f, the amount of kinetic energy at the downstream cross-section is less than 1% of total energy (Figure 13a, b, c). These new results demonstrate a key role for channel non-uniformity in controlling the diverse conditions found in the vicinity of natural river steps, in contrast to the limited conditions reported for engineered steps.

3.3 Varying Upstream Channel Geometry

A comparison among results for different sets of f_{up} and b_{up} combinations (Figures 11 and 12) shows that the standard concept of how steps function breaks down when at-a-station hydraulic geometry is not dominated by depth-responsiveness, i.e., when the value of *f* is low. Because the sensitivity of the system to *f* and *b* values is co-dependent on the *fratio*, the results are explained for specified example *fratio* values. The most extreme condition examined in which the standard conceptual model breaks down is the case when *fratio*≥1.5 (Figure 11, circles). Under this condition, the hydraulic jump is pushed downstream of the step toe at high *(H+P)/H* values for all channel geometries. As *(H+P)/H* decreases, the jump becomes increasingly emergent (i.e. the supercritical zone downstream of the step toe becomes longer) until no jump is present and the flow remains supercritical throughout the downstream section. The threshold for supercriticality depends on the channel geometry, occurring at lower *(H+P)/H* ratios as either *f* or *b* increases. Thus for *fratio*≥1.5, the hydraulic jump regime is insensitive to the absolute values of *f* and *b*. It is sensitive, however, in terms of energy loss and kinetic energy (Figure 12, 13). For *fratio*≥1.5, the system in general incurs more head loss for higher values of *f* and *b*; except for cases in which *b*≥0.4, then the system exhibits greater head loss for decreasing *f* values. This pattern corresponds with the general decrease in kinetic energy as *f* and/or *b* increase.

The behavior of the hydraulic jump regime as a function of *f* and *b* values when *fratio*=1.25 (Figure 11, squares) appears to be similar to that described above, when both *f* and *b* values are low. Under that condition, the flow becomes fully supercritical throughout the downstream section for low *(H+P)/H* values. At high *f* and *b* values, however, the jump exists as a pushed-off jump throughout the range of *(H+P)/H* values. The head loss for systems with *fratio*=1.25 responds similarly to *fratio*≥1.5 systems described above.

In contrast to the insensitivity of the jump emergence regime to upstream *f* and *b* values when *fratio*≥1.0, the fundamental behavior of the hydraulic jump regime shows strong sensitivity to those variables when *fratio*≤1.0. When *f*=0.4 and *fratio*=0.75, the hydraulic jump submerges increasingly fast as a function of decreasing *(H+P)/H*, regardless of the value of *b*. A similar trend is evident when *b*=0.4 and *fratio*=0.75, except when *f*=0.2. In that case the depth-response is weak enough that he just transitions from a pushed-off to an optimum jump condition, but not to a submerged jump (Figure 11i). Holding *f*=0.2 and *fratio*=0.75, as b decreases from 0.4 to 0.2, the geometric effect is to bend the channel from convex-up to triangular, but also to strongly raise the stage-dependence of channel slope and/or roughness. These changes enable the downstream cross-section to transport water away faster, which lowers the tailwater depth and emerges of the hydraulic jump for any given *(H+P)/H*. (Figure 11g-i). The head loss when *fratio*=0.75 tends to decrease with increasing upstream *b* or *f* values (Figure 12), since the tailwater depth is higher at those higher exponent values.

When *fratio*=0.5 (Figure 11, triangles), the channel choking (i.e. upstream submergence due to downstream controls) is extreme enough that the nonlinear rate of submergence increases for all values of *b* and *f* to the point that no surface feature is present when *(H+P)/H*=2 unless *f* and *b* are both ≤0.2 (Figure 11g). In that case, the at-a-station hydraulic geometry requires that most of the response to increasing discharge goes to increasing flow velocity, thereby holding off complete drowning of the step. The head loss decreases rather quickly compared to the other *fratio* systems with decreasing *(H+P)/H* values. The response of the head loss is, however, insensitive to varying *b* and *f* values, except for the extreme lower *b* and *f* values (≤2) (Figure 12g). The head loss response mimics the hydraulic jump regime response.

3.4 Model Sensitivity to Geometric Coefficients

The impact of the hydraulic geometry coefficients, a and c, on step mechanics is similar to that reported for manipulations of the *fratio* (Figures 14-17), and is consistent with intuition based on the geometric explanations provided in sections 2.2, 2.3, 3.1, and 3.2. The step response to only variations in geometric coefficients is evident in the results for *fratio*=1 (Figures 14-17, diamonds). For example, when $f_{up}=b_{up}=0.2$ and *fratio*=1, the hydraulic jump regimes become more supercritical as either a or c decrease with increasing discharge (i.e. decreasing $(H+P)/H$) (Figure 14). A similar effect was described as either b or f decreased, while coefficients were held constant (Figure 11). A decrease in either coefficient while holding the other constant and the exponents constant requires an increase in the coefficient k. Physically, that means that the channel is steeper and/or smoother, which enables water to transport out of the step region faster, lowering tailwater depth and emerging the jump regime. The same emergence response of hydraulic jump regime to decreasing a and/or c is evident regardless of *fratio* (Figure 14). These patterns were also observed when holding coefficients constant and varying exponents (Figure 11).

When $f_{up}=b_{up}=0.4$, the sensitivity of the model to the coefficients is quite dampened (Figure 16), as compared to the case when $f_{up}=b_{up}=0.2$. For all combinations of a and c tested at these higher exponent values, the hydraulic jump submerged with increasing discharge when *fratio*<0.9. These results show that channels whose energy slope and bed roughness exhibit a sensitive discharge-dependence will be more sensitive to the exact values of the coefficients than channels whose primary discharge sensitivity is exhibited in depth and/or width.

The similarity of the response of the hydraulic jump regimes to changes in the coefficients versus the exponents of equation (7) holds in the energy loss relations as well (e.g. compare

Figures 12, 15, and 17). When f_{up}=b_{up}=0.2, energy loss is lower for higher coefficient values, since tailwater depth and velocity are lower (Figure 15). When f_{up}=b_{up}=0.4, the range of variability in energy loss as a function of coefficient values is less than when f_{up}=b_{up}=0.2 (Figure 17). These results confirm that either the geometric coefficients or exponents can affect the step response, even though they do so differently – by stretching versus bending of the channel cross-section.

4. Discussion

4.1 Energy, Velocity, and Erosion

For any set of model parameters, the results revealed an inverse relation between velocity at the downstream cross-section and energy loss through the step for a given *fratio* (Figure 13). This finding has ramifications for step erosion mechanisms. At low discharge, step height is relatively high and energy dissipation is in the range of 80-95% of total energy. As water goes over the brink, it accelerates and hits the bed downstream of the step toe. For a vertical step, the angle of the nappe profile is steepest at the lowest discharge [*Pasternack et al.,* 2006], which facilitates direct hydraulic erosion [*USBR, 1948a*]. For the range of hydraulic geometry coefficients and exponents explored, the hydraulic jump regime for low discharge is predominantly pushed off or optimal jump, meaning that the falling jet can go through the tailwater, impact the bed, and cause erosion, promoting plunge-pool formation. However, since the specific energy (H) is low at low discharge, the velocity of the water as it goes over the brink is relatively low, and even with acceleration it remains relatively low at the step toe compared to that at higher H. When the water reaches the downstream cross-section, its velocity is very low, since most energy was dissipated (Figure 13). As discharge increases, upstream velocity,

tailwater depth, and tailwater velocity all increase, while nappe profile angle becomes more horizontal and energy loss decreases, all driven by higher specific energy. Depending on the *fratio*, the hydraulic jump regime may become more emergent or more submerged. Different scour mechanisms appear to exist for the different hydraulic jump regimes [*Pasternack et al., 2007*], but insufficient literature exists to compare and contrast the relative magnitude of scour under pushed off versus optimum jump conditions. However, once a jump is drowned, both jet impingement and lift-stress variation on the bed likely decrease. Higher energy loss, higher velocity at the step toe, and jump emergence promote bed scour, while lower energy loss, jump submergence, and a more horizontal nappe profile diminish it. Therefore, the mechanisms and magnitude of scour vary substantially for a given channel configuration as discharge changes.

Compared to the velocity, energy loss, and implied scour mechanics at an individual step, there is a highly significant effect of changing channel configuration. For all sets of model parameters explored, an increase in the *fratio* (or an equivalent change to geometric coefficients) for a given level of tailwater kinetic energy causes a dramatic increase in energy loss and keeps the tailwater velocity high (Figure 13). For example, when kinetic energy is held at 5% of total energy and the other parameters are as given for Figures 9e and 10e, energy loss increases from zero for a *fratio* of 0.5 to 63% of total energy for a *fratio* of one to 76% for a *fratio* of 1.5 (Figure 18). As the *fratio* and energy loss increase, the hydraulic jump regime emerges, while the nappe profile angle remains the same, since H is the same. In this case, different factors and scour mechanisms are working synergistically to promote bed scour. Overall, the model results demonstrate that variation in channel configuration is a powerful variable controlling scour mechanisms at river steps.

4.2 Knickpoints at Canyon Entrances

One physiographic domain in which knickpoints are common is the transitional canyon between high-elevation plateaus and lowlands. In such regions, there exist observations of knickpoints occurring at the upstream limit of the canyon, right at the transition point where valley and channel width suddenly changes [e.g., *Snyder and Kammer, 2008*]. Landscape evolution models of this domain that simulate plateau retreat by computing channel scour as a function of local slope and basin area predict higher rates of retreat during higher flows. However, the results of this study indicate that the exact opposite could hold, or scour rates could just be independent of discharge. Specifically, a knickpoint at the transition from a high plateau to a bedrock canyon exhibits valley constriction through the step unit. As discharge increases during an overbank event, the tailwater depth would quickly increase and drown the step, neutralizing the most effective scour mechanisms acting on the step toe. If the step is too high to completely submerge, it would at least drown enough to protect the bed from both hydraulic jet scour and bedload-impact scour. Thus, the geomorphically significant example of plateau-to-canyon transitions illustrates the importance of the new model relative to the existing algorithms used in landscape evolution modeling. Scour at knickpoints in bedrock channels is definitely not a simple power function of slope and basin area.

4.3 Model Applications

Investigation of the fluid mechanics at river steps in non-uniform channels using a parsimonious semi-analytical model revealed important non-classical behavior governing the fundamental nature of river steps. Although the model was generalized for broad scientific inquiry, model parameterization for a specific local site would enable its use for a wide range of

management and engineering applications. For a specified site, such parameterization would entail observing channel width and depth upstream and downstream of the step over the range of flows under the baseline condition. Once the local flow-geometry relations are known, then the model becomes easily testable for any site since the only independent input variable needed is the upstream flow depth. Theoretical jump regimes and energy losses could then be compared to experimental or observed conditions. After satisfactory validation of the local model, alternative modifications to the channel geometry could be tested with the model to evaluate the resulting hydraulic jump and energy dissipation regimes relative to the desired goals. Common goals typically involve reducing swimmer or boater drowning hazard, decreasing the rate of knickpoint migration in gullies, and creating exciting recreational whitewater parks.

Leutheusser and Birk [1991] described the drowning hazard posed by overflow hydraulic structures that have a drowned jump (a.k.a. "plunging nappe") and they analyzed the engineering requirements to avoid this hazard. The same hazard exists at many natural steps as well. The design goal to avoid the hazard is to ensure that the step has any other hydraulic jump regime over the range of discharge and tailwater depth conditions that occur there. The solution provided by *Leutheusser and Birk* [1991] only allows for adjustment of step height. Using the new model proposed herein, the same hazard avoidance can be achieved using a variety of geometric adjustments. For situations where step height could not be modified, one solution would be increase the *fratio* of the channel to keep the step toe in the optimum jump condition over the range of discharges expected.

Although the model does not directly predict scour and knickpoint migration rates at this time, it does provide the basis for inference and channel design. A key advantage of linking scour to energy dissipation instead of drag force is that existing equations used to predict scour using

the latter approach have been shown to perform poorly [*Pasternack et al.,* 2007], because they do not account for the mechanics and trade-offs discussed in section 4.1. In contrast, this new numerical model predicting energy dissipation does account for different processes, including the hydraulic jump regime. According to the model, the higher the *fratio* for a knickpoint, then the more the channel morphology is promoting higher energy dissipation (Figure 12) and thus higher rates of toe scour and knickpoint migration related to this process. To reduce the rate of knickpoint migration in that case, the channel manipulation would be the exact opposite of that for drowning hazard mitigation. By decreasing the *fratio* at a site, the magnitude of energy dissipation at the knickpoint would be decreased for a given tailwater velocity (Figures 12, 18) and the hydraulic jump would be more submerged (Figure 11), for any given discharge. The utility of this solution depends on the actual *fratio* at a knickpoint and the degree to which a site can be re-engineered.

A third example where this model would be of value is in the construction of increasingly popular, recreational whitewater parks. The primary engineering feature used repetitively in such parks is a channel constriction at the step to produce the desired standing wave or hydraulic jump for canoe and kayak acrobatics (Figure 19). Presently such features are designed based on practitioner experience, but the model could be used to accurately predict and control what the jump regime will be in advance as a cost-saving measure. Similar applications are readily apparent for dam removal, river rehabilitation, and fish passage – all situations in which human safety is jeopardized by the unknown hydraulic jump regime and geomorphic unit instability associated with step scour that is not accurately predicted by accounting for the scour associated with energy dissipation at the step.

4.4 Roadmap for Step Theory Advancement

The underlying assumptions and limitations of the new model presented in this study have been described in detail throughout. Although this study explored a wide range of model parameters, there exists a dearth of data on the hydraulic geometry of channels in the vicinity of knickpoints. The exact relation between *fratio* and *bratio* in bedrock channels is unknown. The relative abundance of steps with different *fratios*, perhaps as a function of uplift rate and geology, is unknown. Overall, a new examination and appreciation of the real diversity in natural river steps needs to replace existing models based on processes in alluvial rivers, gullies, and man-made spillways.

The biggest deficiency in the model at this time is in the hydraulic jump regime equations (15)-(18), which are only strictly valid for an ogee-crested, rectangular 2-D overfall. The delineation between optimum jump and drowned jump regimes suggestbed by *USBR* [1948b] appears highly subjective. Also, the thresholds do not delineate the standing wave regime. Consequently, this theoretical study indicates that future research into the hydraulic geometry of step units in bedrock rivers and the dynamics of hydraulic jump regimes for different archetypal steps should be prioritized.

Beyond the numerical model, key areas of future research are suggested by the conceptual framework (Figure 1). Most important would be to quantify the role of hydraulic jump regime and energy dissipation in step morphodynamics. In the past, studies have focused on the role of the hydraulic jet in scouring the plunge-pool [*Mason and Arumugam,* 1985*; Bormann and Julien,* 1991]. Some studies have also demonstrated the importance of pressure fluctuations and lift in scour below steps [*Fiorotto and Rinaldo,* 1992*; Fiorotto, V., Salandin,* 2000*; Pasternack et al.*, 2007], though not accounting for scour associated with bedload-impact. As airborne laser swath

mapping provides meter-scale resolution of topography in otherwise inaccessible canyons, we conjecture that it will be possible for landscape evolution models to incorporate the knickpoint mechanics associated with channel non-uniformity. Other factors in the conceptual framework that could be addressed relatively easily include step roughness and wind.

5. Conclusions

The effect of varying channel geometry upstream and downstream of a river step on hydraulic jump regime and energy dissipation has not previously been investigated. This research has quantified the roles that hydraulic geometry and discharge have in determining the hydraulic jump regime and energy dissipation at river steps using a parsimonious model. For a given discharge and step morphology, an increase in the *fratio* leads to an increasingly emergent hydraulic jump. Channel non-uniformities that exhibit an *fratio*>1.0 tend to be relatively insensitive to changes in the *f* or *b* parameters in terms of the hydraulic jump regime, existing as a pushed-off jump or supercritical flow for the whole range of *(H+P)/H* values. However, these channel non-uniformities exhibit higher energy loss through a step as *f* or *b* increases. For channel non-uniformities with an *fratio*<1.0, there exists a strong sensitivity to changes in both *f* and *b* values in terms of the hydraulic jump regime ranging from a pushed-off jump to a completely drowned-out jump. The head loss of these systems decreases with either increasing *f* or *b* values. For non-uniformities with *fratio*>1.0, head losses are high over the whole *(H+P)/H* range. For non-uniformities with *fratio*<1.0, flow becomes choked and head losses decrease significantly as *(H+P)/H* decreases. Regardless of channel geometry, head losses due to potential energy losses dominate the flow regime at high relative step heights.

Limitations in the model show that as the ratio h_d/H approaches zero, the simple hydraulic geometry equations no longer apply at the upstream cross-section, because the downstream depth acts as a control on the upstream depth. Because of the interplay between flow, channel geometry, and geological resistance, step toe emergence with high energy dissipation can induce scour and plunge pool formations, limiting the abundance of natural emerged jump regimes at bedrock steps. It may be that using a cross-section to characterize the downstream control on the step toe is inadequate, necessitating a 3-D topographic and hydrodynamic modeling framework. However, the parsimony of the analytical approach presented herein provides a reasonable predictive foundation for further analytical investigation.

A better understanding of hydro-geomorphic processes in mountain rivers, particularly at river steps, would provide advancement in the understanding of mountain river fluid mechanics, aquatic ecology, and channel evolution. Such improved understanding can aid in determining the impacts of channel engineering projects and can provide guidance to river restoration and urban stream rehabilitation efforts. Previous research has typically ignored the relevance of hydraulic jumps within channel evolution models. Since hydraulic jump regimes can be associated with steps of any size, including those induced by large wood jams and gravel bars, a better understanding of complex step processes can contribute to a better understanding of many channel features.

6. Acknowledgements

This research was funded by the Hydrology Program of the National Science Foundation under Agreement number EAR-0207713. Any opinions, findings, and conclusions or recommendations expressed in this material are those of the authors and do not necessarily reflect the views of the

National Science Foundation. We thank Greg Tucker, Itai Haviv, Paul Carling, Kurt Frankel, Noah Snyder, Marc Parlange, and anonymous reviewers for helpful feedback.

Notation

a	hydraulic geometry width coefficient
b_{up}	upstream hydraulic geometry width exponent
b_{tail}	downstream hydraulic geometry width exponent
c	hydraulic geometry depth coefficient
C_b	broad-crested weir discharge coefficient
E	total flow energy
E_{up}	upstream total flow energy
E_{tail}	downstream total flow energy
f_{up}	upstream hydraulic geometry depth exponent
f_{tail}	downstream hydraulic geometry depth exponent
$fratio$	ratio of f_{up} to f_{tail}
Fr	Froude number
g	gravitational constant
H	specific energy upstream of step
h_b	flow depth at brink of step
h_c	critical depth
h_d	submergence variable of hydraulic jump
h_H	flow depth above step crest datum
h_{up}	upstream flow depth
h_{tail}	downstream flow depth
h_{toe}	flow depth at toe of hydraulic jump
h_L	head loss
h_v	velocity head
h_{v_up}	upstream velocity head
h_{v_tail}	downstream velocity head
k_{up}	upstream hydraulic geometry velocity coefficient
k_{tail}	downstream hydraulic geometry velocity coefficient
m_{up}	upstream hydraulic geometry velocity exponent
m_{tail}	downstream hydraulic geometry velocity exponent
P	step height
Q	volumetric discharge
q	specific discharge
v	flow velocity
w	flow width

7. References

Ackers, P., W. White, J. Perkins, and A. Harrison (1978), *Weirs and Flumes for Flow Measurement*, 327 pp., John Wiley & Sons, Chicester, NY.

Alexandrowicz, Z. (1994), Geologically controlled waterfall types in the Outer Carpathians, *Geomorphology*, *9*(2), 155-165.

Alonso, C.V., S.J. Bennett, and O.R. Stein (2002), Predicting head cut erosion and migration in concentrated flows typical of upland areas, *Water Resour. Res. 38*(12), 1303, doi:10.1029/2001WR001173.

Andrews, E.D. (1984), Bed-material entrainment and hydraulic geometry of gravel-bed rivers in Colorado, *Geol. Soc. Am. Bull.*, *95*(3), 371-378.

Balachandar, R., J.A. Kells, and R.J. Thiessen (2000), The effect of tailwater depth on the dynamics of local scour, *Can. J. Civil Eng.*, *27*(1), 138-150.

Bennett, S.J., C.v. Alonso,, S.N. Prasad, and M.J.M. Römkens (2000), Experiments on headcut growth and migration in concentrated flows typical of upland areas, *Water Resour. Res. 36*(7), 1911-1922.

Betson, R.P. (1979), A geomorphic model for use in streamflow routing, *Water Resour. Res.*, *15*(1), 95-101.

Bollaert, E., and A. Schleiss (2003), Scour of rock due to the impact of plunging high velocity jets Part I: A state-of-the-art review, *J. Hydraul. Res., 41*(5), 451-464.

Bormann, N.E., and P.Y. Julien (1991), Scour downstream of grade-control structures, *J. Hydraul. Eng. 117*(5), 579-594.

Carling, P.A. (1995), Flow-separation berms downstream of a hydraulic jump in a bedrock channel, *Geomorphology*, *11*(3), 245-253.

Chanson, H. (1999), *The Hydraulics of Open Channel Flow: An Introduction*, 495 pp., Arnold Publishing, London, England.

Chanson, H. (2002), *The Hydraulics of Stepped Chutes and Spillways*, 384 pp., A.A. Balkema Publishers, Lisse, Netherlands.

Chaudry, M.H. (1993), *Open-Channel Flow*, 483 pp., Prentice Hall, Englewood Cliffs, NJ.

Dingman, S.L. (2007), *Analytical derivation of at-a-station hydraulic-geometry relations, J. Hydrol., 334,* 17-27.

Drury, G.H. (1976), Discharge prediction, present and former, from channel dimensions, *J. Hydrol.*, *30*, 219-245.

Falvey, H.T. (2003), *Hydraulic Design of Labyrinth Weirs*, 162 pp., American Society of Civil Engineers, Reston, VA.

Fiorotto, V., and A. Rinaldo (1992), Fluctuating uplift and ling design in spillway stilling basins, *J. Hydraul. Eng.*, *118*(4), 578-596.

Fiorotto, V., and P. Salandin (2000), Design of anchored slabs in spillway stilling basins, *J. Hydraul. Eng., 126*(7), 502-512.

Flores-Cervantes, J.H., E. Istanbulluoglu, and R.L. Bras (2006), Development of gullies on the landscape: A model of headcut retreat resulting from plunge pool erosion, *J. Geophys. Res.*, *111*, F01010, doi:10.1029/2004JF000226.

Frankel, K.L., F.J. Pazzaglia, and J.D. Vaughn (2007), Knickpoint evolution in a vertically bedded substrate, upstream-dipping terraces, and Atlantic slope bedrock channels, *Geol. Soc. Am. Bull., 119*, 476-486.

Garde, R.J., and K.G. Ranga Ragu (1985), *Mechanics of Sediment Transportation and Alluvial Stream Problems*, John Wiley & Sons, New York.

Gasparini, N.M., K.X. Whipple, and R.L. Bras (2007), Predictions of steady state and transient landscape morphology using sediment-flux-dependent river incision models, *J. Geophys. Res., 112*, F03S09, doi: 10.1029/2006JF000567.

Grant, G.E. (1997), Critical flow constrains flow hydraulics in mobile-bed streams: A new hypothesis, *Water Resour. Res.*, *33*(2), 349-358.

Hanson, G.J., K.M. Robinson, and K.R. Cook (1997). Headcut migration analysis of a compacted soil, *Trans. ASAE 40*(2), 355–361.

Hayakawa, Y., and Y. Matsukura (2003), Recession rates of waterfalls in Boso Peninsula, Japan, and a predictive equation, *Earth Surf. Proc. Landf., 28*(6), doi:10.1002/esp.519.

Henderson, F.M. (1966), *Open Channel Flow*, p. 79-228, Macmillan, New York, New York.

Kieffer, S.W. (1987), The rapids and waves of the Colorado River, Grand Canyon, Arizona, *U.S. Geol. Surv. Open-file Report #87-096*.

Lenzi, M.A., A. Marion, F. Comiti, and R. Gaudio (2002), Local scouring in low and high gradient streams at bed sills, *J. Hydraul. Res.*, *40*(6), 731-739.

Lenzi, M.A., A. Marion, and F. Comiti (2003), Local scouring at grade-control structures in alluvial mountain rivers, *Water Resour. Res.*, *39*(7), doi:10.1029/2002WR001815.

Leopold, L.B., and T.J. Maddock (1953), Hydraulic geometry of stream channels and some physiographic implications, *U.S. Geol. Surv. Prof. Pap., 252*, 55 pp.

Leutheusser, H.J., and W.M. Birk (1991), Downproofing of low flow structures, *J. Hydraul. Eng.*, *117*(2), 205-213.

Marion, A., M. Tregnaghi, and S. Trait (2006), Sediment supply and local scouring at bed sills in mountain streams, *Water Resour. Res.*, 42, W06416, doi:10.1029/2005WR004124.

Mason, P.J., and K. Arumugam (1985), Free jet scour below dams and flip buckets, *J. Hydraul. Eng. 111*(2), 220-235.

McCarthy, M.F., and P.M. O'Leary (1978), The growth and decay of a hydraulic jump, *J. Hydrol.*, *39*(3-4), 273-285.

Montgomery, D.R., and J.M. Buffington (1997), Channel-reach morphology in mountain drainage basins, *Geol. Soc. Am. Bull.*, *109*(5), 596-611.

Moore, W.L. (1943), Energy loss at the base of a free overfall, *Trans. ASCE, 108*, 1343-1360.

Mossa, M., A. Petrillo, and H. Chanson (2003), Tailwater level effects on flow conditions at an abrupt drop, *J. Hydraul. Res.*, *41*(1), 39-51.

Munson, B.R., D.F. Young, and T.H. Okiishi (2006), *Fundamentals of Fluid Mechanics*, 5th ed., 769 pp., John Wiley & Sons, Inc., Hoboken, NJ.

Negm, A.M. (2000), Generalization of Belanger Equation, *Proc. 4th International Conference on Hydro-Science and -Engineering-2000*, Sept 26-29, Seoul, Korea.

Ohtsu, I., Y. Yasuda, and M. Ishikawa (1999), Submerged hydraulic jumps below abrupt expansions, *J. of Hydraul. Eng.*, *125*(5), 492-499.

Pasternack, G.B., C.R. Ellis, K.A. Leier, B.L. Vallé, and J.D. Marr (2006), Convergent hydraulics at horsehoe steps in bedrock rivers, *Geomorphology*, doi:10.1016/j.geomorph.2005.08.022.

Pasternack, G.B., C.R. Ellis, and J.D. Marr (2007), Jet and hydraulic jump near-bed stresses below a horseshoe waterfall, *Water Resour. Res.*

Ram, K.V.S., and R. Prasad (1998), Spatial B-jump at sudden channel enlargements with abrupt drop, *J. Hydraul. Eng.*, *124*(6), 643-646.

Rhoads, B.L. (1991), A continuously varying parameter model of downstream hydraulic geometry, *Water Resouc. Res.*, *27*(8), 1865-1872.

Robinson, K.M, and G.J. Hanson (1996), Gully headcut advance, *Trans. ASAE, 39*(1), 33-38.

Seidl, M.A., and W.E. Dietrich (1992), The problem of channel erosion into bedrock, in *Functional Geomorphology, Catena Suppl., 23*, 101-124.

Singh, V.P. (2003), On the theories of hydraulic geometry, *Int. J. Sediment Res.*, *18*(3), 196-218.

Sinha, S.K., F. Sotiropoulos, and A.J. Odgaard (1998), Three-dimensional numerical model for flow through natural rivers, *J. Hydraul. Eng.*, *124*(1), 13-24.

Sklar, L.S., and W.E. Dietrich (2004), A mechanistic model for river incision into bedrock by saltating bed load, *Water Resour. Res. 40*, W06301, doi:10.129/2003WR002496.

Slattery, M.C., and R.B. Bryan (1992), Hydraulic conditions for rill incision under simulated rainfall: A laboratory experiment, *Earth Surf. Proc. Land., 17*, 127-146.

Smart, G.M. (1999), Turbulent velocity profiles and boundary shear in gravel bed rivers, *J. Hydraul. Eng.*, 125, 106-116.

Snyder, N.P., and Kammer, L.L. (2008), Dynamic adjustments in channel width in response to a forced diversion: Gower Gulch, Death Valley National Park, California, *Geology*, 25, 187-190.

Stock, J.D., and D.R. Montgomery (1999), Geologic constraints on bedrock incision using the stream power law, *J. Geophys. Res., 104*(B3), 4983-4993.

Smith, C.D. (1976), Hydraulic design for an outlet structure, Proc. Symp., Waterways, Harbors, & Coastal Engr. Div., ASCE, on Inland Waterways for Navigation, Flood Control, and Water Diversions, *2*, 1179-1198.

Stein, O.R., P.Y. Julien (1993), Criterion delineating the mode of headcut migration, *J.Hydraul. Eng. 119*(1), 37-50.

Stein, O.R., P.Y. Julien, and C.V. Alonso (1993), Mechanics of jet scour downstream of a headcut, *J. Hydraul. Res. 31*(6), 723-738.

Stein, O.R., and D.A. LaTray (2002), Experiments and Modeling of Headcut Migration in Stratified Soils, *Water Resour. Res. 38*(12), 1284:doi:10.1029/2001WR001166.

Stewardson, M. (2005), Hydraulic geometry of stream reaches, *J. Hydrol.*, *306*(1-4), 97-111.

Valle, B.L., and G.B. Pasternack (2002), TDR Measurements of Hydraulic Jump Aeration in the South Fork of the American River, CA. *Geomorphology* 42, 153-165.

Valle, B.L., and G.B. Pasternack (2006a), Air concentrations of submerged and unsubmerged hydraulic jumps in a bedrock step-pool channel, *J. Geophys. Res.* 111, F03016, doi:10.1029/2004JF000140.

Vischer, D.L., and W.H. Hager (1998), *Dam Hydraulics*, John Wiley & Sons, New York, NY.

White, M.P. (1943), Energy loss at the base of a free overfall- discussion, *Trans. ASCE, 108*, 1361-1364.

Wilcock, D.N. (1971), Investigation into the relations between bedload transport and channel shape, *Geol. Soc. Am. Bull.*, *82*, 2159-2176.

Wohl, E.E., and T. Grodek (1994), Channel bed-steps along Nahal Yael, Negev Desert, Israel, *Geomorphology*, *9*(2), 117-126.

U.S. Bureau of Reclamation (1948a), Model studies of spillways, Boulder Canyon Project Final reports, *Part VI-Hydraulic Investigations, Bulletin 1*.

U.S. Bureau of Reclamation (1948b), Studies of crests for overfall dams, Boulder Canyon Project Final Reports, *Part VI-Hydraulic Investigations, Bulletin 3*.

Figure Captions

Figure 1 - Flowchart showing interrelationships between dependent and independent processes at river steps. Rhombi are external independent processes. Bold arrows indicate processes discussed herein.

Figure 2 – Longitudinal schematic of an idealized step showing a submerged jump illustrating parameters used in the model. Not to scale to permit notation (See notation list).

Figure 3 – Physical interpretation of hydraulic geometry exponent values for a cross-section in a single-threaded stream. Shaded region is where $b>f$.

Figure 4 – Sensitivity analysis illustrating the similar effects on channel width of varying either (A) the coefficient a or (B) the exponent b in equation (7a), while holding the other constant.

Figure 5 – Illustration of the channel non-uniformity through a reach with a river step where the $f_{ratio}<1$. Widths, depths, and shapes are roughly to scale, but are not mapped quantitatively. Depth and width values for values of (H+P)/H equal to 5.81 (i.e. low discharge) and 1.98 (i.e. high discharge) are shown for $f_{up}=b_{up}=0.4$ and $fratio=0.5$.

Figure 6 – Example of a step unit with *f>b* and *fratio<1* showing channel constriction through the domain. Upper South Fork Snoqualmie River, California, looking upstream

Figure 7 – Illustration of the channel non-uniformity through a reach with a river step where the f_{ratio}>1. Widths, depths, and shapes are roughly to scale, but are not mapped quantitatively. Depth and width values for values of (H+P)/H equal to 5.81 (i.e. low discharge) and 1.98 (i.e. high discharge) are shown for f_{up}=b_{up}=0.4 and *fratio*=0.5.

Figure 8 – Example of a step unit with *f>b* and *fratio>1* showing channel expansion through the domain. Upper South Fork Blackwood Creek, California, looking upstream.

Figure 9 - Generalized hydraulic jump regimes in reference to dimensionless upstream energy and downstream submergence, as derived from *USBR [1948b]*.

Figure 10 – Width to depth ratios at the downstream cross section as a function of dimensionless upstream energy illustrating that the f_{ratio} effectively controls channel constriction and expansion as a function of discharge through a reach with a river step.

Figure 11 – Hydraulic jump regime model results and sensitivity analysis for the ranges of f_{up}, b_{up}, and *fratio* explored. The *f* and *b* values stated refer to upstream condition. Solid lines delineate hydraulic jump regimes.

Figure 12 - Energy dissipation model results and sensitivity analysis for the ranges of f_{up}, b_{up}, and *fratio* explored. The *f* and *b* values stated refer to upstream condition.

Figure 13 – Energy loss through the step and kinetic energy at the downstream cross-section had an inverse relation for any given set of parameters explored.

Figure 14 – Hydraulic jump regime model results and sensitivity analysis for the ranges of a_{up}, c_{up}, and *fratio* explored with f_{up}=b_{up}=0.2. The *a* and *c* values stated refer to upstream condition. Solid lines delineate hydraulic jump regimes.

Figure 15 – Energy dissipation model results and sensitivity analysis for the ranges of a_{up}, c_{up}, and *fratio* explored with $f_{up}=b_{up}=0.2$. The *a* and *c* values stated refer to upstream condition.

Figure 16 – Hydraulic jump regime model results and sensitivity analysis for the ranges of a_{up}, c_{up}, and *fratio* explored with $f_{up}=b_{up}=0.4$. The *a* and *c* values stated refer to upstream condition. Solid lines delineate hydraulic jump regimes.

Figure 17 – Energy dissipation model results and sensitivity analysis for the ranges of a_{up}, c_{up}, and *fratio* explored with $f_{up}=b_{up}=0.4$. The *a* and *c* values stated refer to upstream condition.

Figure 18 – Head loss through a river step for a given magnitude of tailwater velocity is higher for reaches with a higher *fratio*. Relation shown is for $f_{up}=b_{up}=0.25$, $a_{up}=a_{tail}=9.74$, $c_{up}=c_{tail}=0.51$, and 5% of total energy at the downstream cross-section exists as kinetic energy.

Figure 19 – Example of engineered step with hydraulic jump in a whitewater park. Lyons Play Park, St. Vrain River, Lyons, Colorado.

Table Captions

Table 1 - Values used in sensitivity analysis of the effect of hydraulic geometry exponents on step hydraulics

Table 1. Values used in sensitivity analysis of the effect of hydraulic geometry exponents on step hydraulics

(a) f_{up}=0.4, b_{up}=0.2

fratio	bratio	f_{tail}	b_{tail}
1.5	0.667	0.267	0.3
1.25	0.800	0.320	0.25
1	1.000	0.400	0.2
0.9	1.111	0.444	0.18
0.75	1.333	0.533	0.15
0.5	2.000	0.800	0.1

(b) f_{up}=0.4, b_{up}=0.25

fratio	bratio	f_{tail}	b_{tail}
1.5	0.667	0.267	0.375
1.25	0.800	0.320	0.313
1	1.000	0.400	0.25
0.9	1.111	0.444	0.225
0.75	1.333	0.533	0.188
0.5	2.000	0.800	0.125

(c) f_{up}=b_{up}=0.4

fratio	bratio	f_{tail}	b_{tail}
1.5	0.667	0.267	0.6
1.25	0.800	0.320	0.5
1	1.000	0.400	0.4
0.9	1.111	0.444	0.36
0.75	1.333	0.533	0.3
0.5	2.000	0.800	0.2

(d) f_{up}=0.25, b_{up}=0.2

fratio	bratio	f_{tail}	b_{tail}
1.5	0.667	0.167	0.3
1.25	0.800	0.200	0.25
1	1.000	0.250	0.2
0.9	1.111	0.278	0.18
0.75	1.333	0.333	0.15
0.5	2.000	0.500	0.1

(e) f_{up}=b_{up}=0.25

fratio	bratio	f_{tail}	b_{tail}
1.5	0.667	0.167	0.375
1.25	0.800	0.200	0.313
1	1.000	0.250	0.25
0.9	1.111	0.278	0.225
0.75	1.333	0.333	0.188
0.5	2.000	0.500	0.125

(f) f_{up}=0.25, b_{up}=0.4

fratio	bratio	f_{tail}	b_{tail}
1.5	0.667	0.167	0.6
1.25	0.800	0.200	0.5
1	1.000	0.250	0.4
0.9	1.111	0.278	0.36
0.75	1.333	0.333	0.3
0.5	2.000	0.500	0.2

(g) f_{up}=b_{up}=0.2

fratio	bratio	f_{tail}	b_{tail}
1.5	0.667	0.133	0.3
1.25	0.800	0.160	0.25
1	1.000	0.200	0.2
0.9	1.111	0.222	0.18
0.75	1.333	0.267	0.15
0.5	2.000	0.400	0.1

(h) f_{up}=0.2, b_{up}=0.25

fratio	bratio	f_{tail}	b_{tail}
1.5	0.667	0.133	0.375
1.25	0.800	0.160	0.313
1	1.000	0.200	0.25
0.9	1.111	0.222	0.225
0.75	1.333	0.267	0.188
0.5	2.000	0.400	0.125

(i) f_{up}=0.2, b_{up}=0.4

fratio	bratio	f_{tail}	b_{tail}
1.5	0.667	0.133	0.6
1.25	0.800	0.160	0.5
1	1.000	0.200	0.4
0.9	1.111	0.222	0.36
0.75	1.333	0.267	0.3
0.5	2.000	0.400	0.2

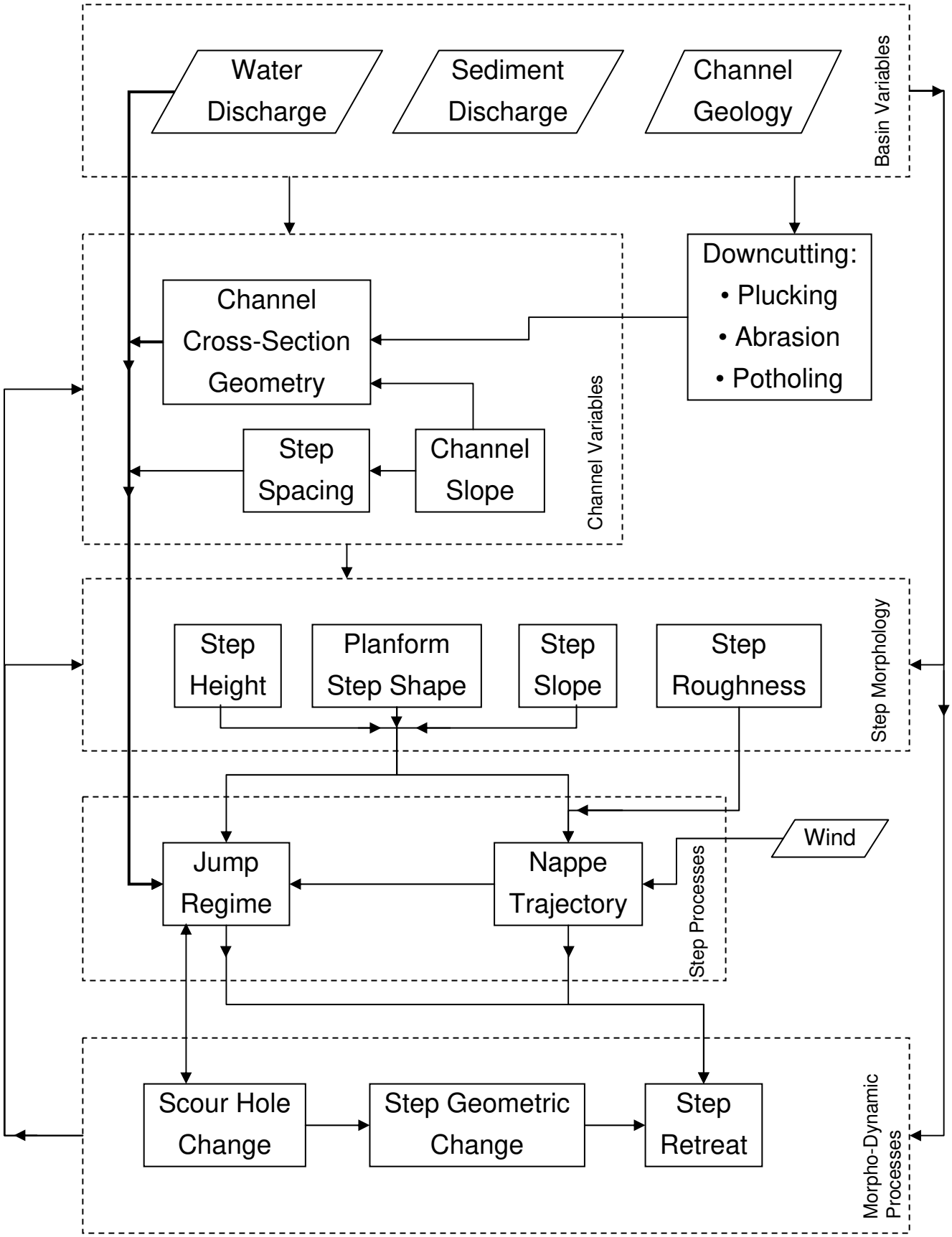
Basin Variables
Water Discharge
Sediment Discharge
Channel Geology
Channel Variables
Downcutting:
• Plucking
• Abrasion
• Potholing
Channel Cross-Section Geometry
Step Spacing
Channel Slope
Step Morphology
Step Height
Planform Step Shape
Step Slope
Step Roughness
Step Processes
Wind
Jump Regime
Nappe Trajectory
Morpho-Dynamic Processes
Scour Hole Change
Step Geometric Change
Step Retreat

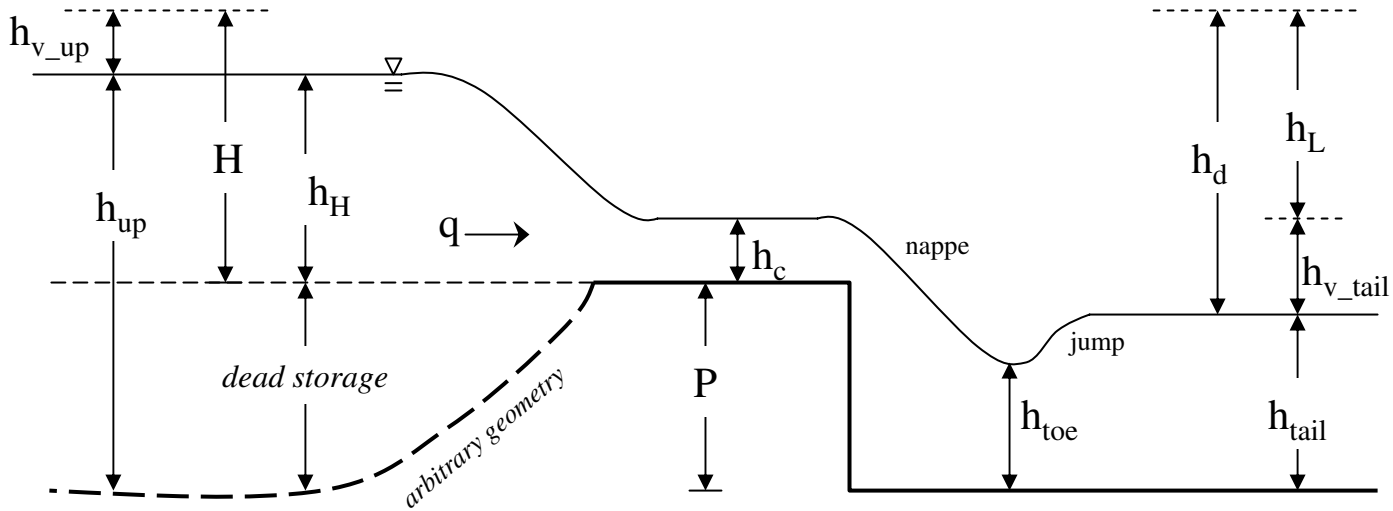
h_{v_up}
H
h_H
h_{up}
q
h_c
nappe
h_d
h_L
h_{v_tail}
jump
dead storage
arbitrary geometry
P
h_{toe}
h_{tail}

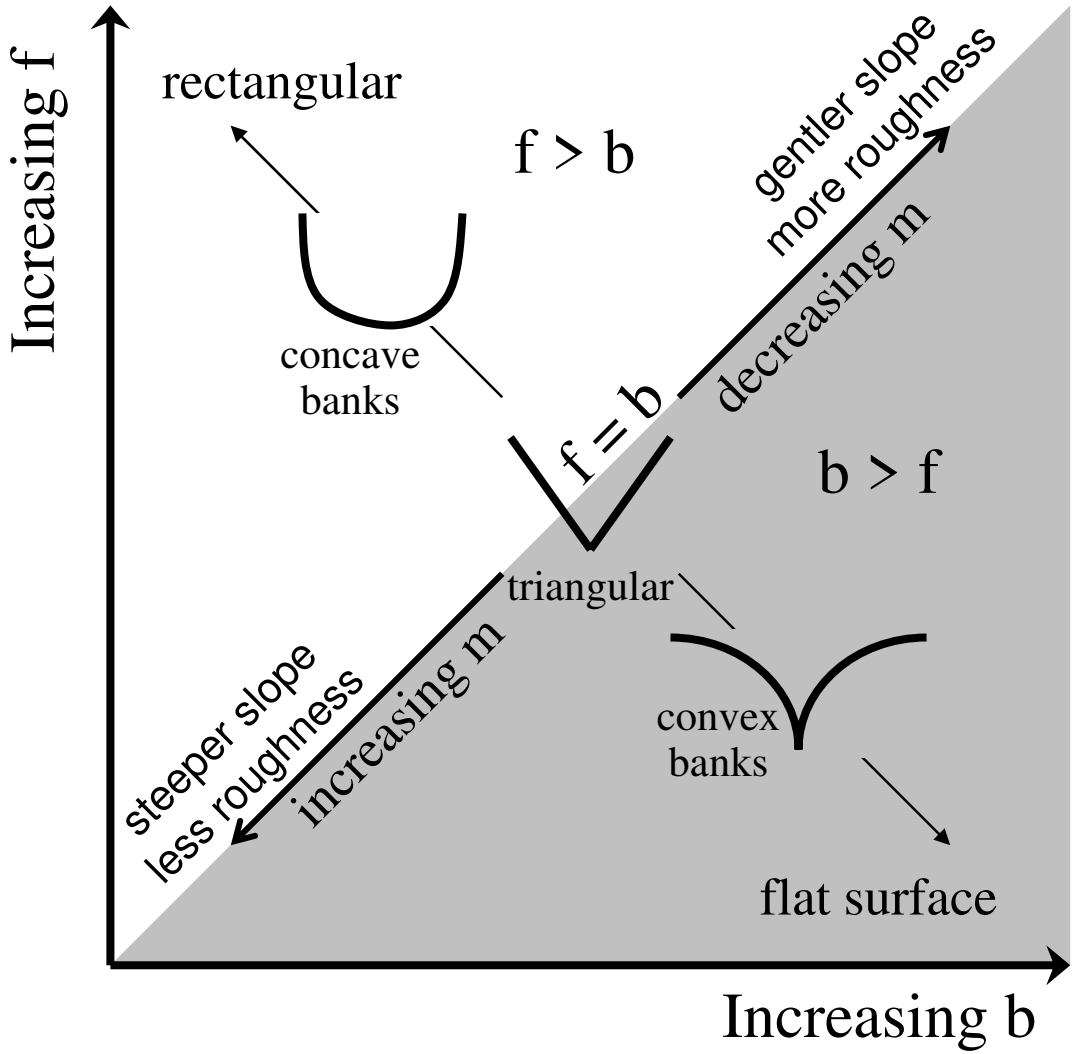
Increasing f
rectangular
f > b
gentler slope
more roughness
decreasing m
concave
banks
f = b
b > f
triangular
steeper slope
less roughness
increasing m
convex
banks
flat surface
Increasing b

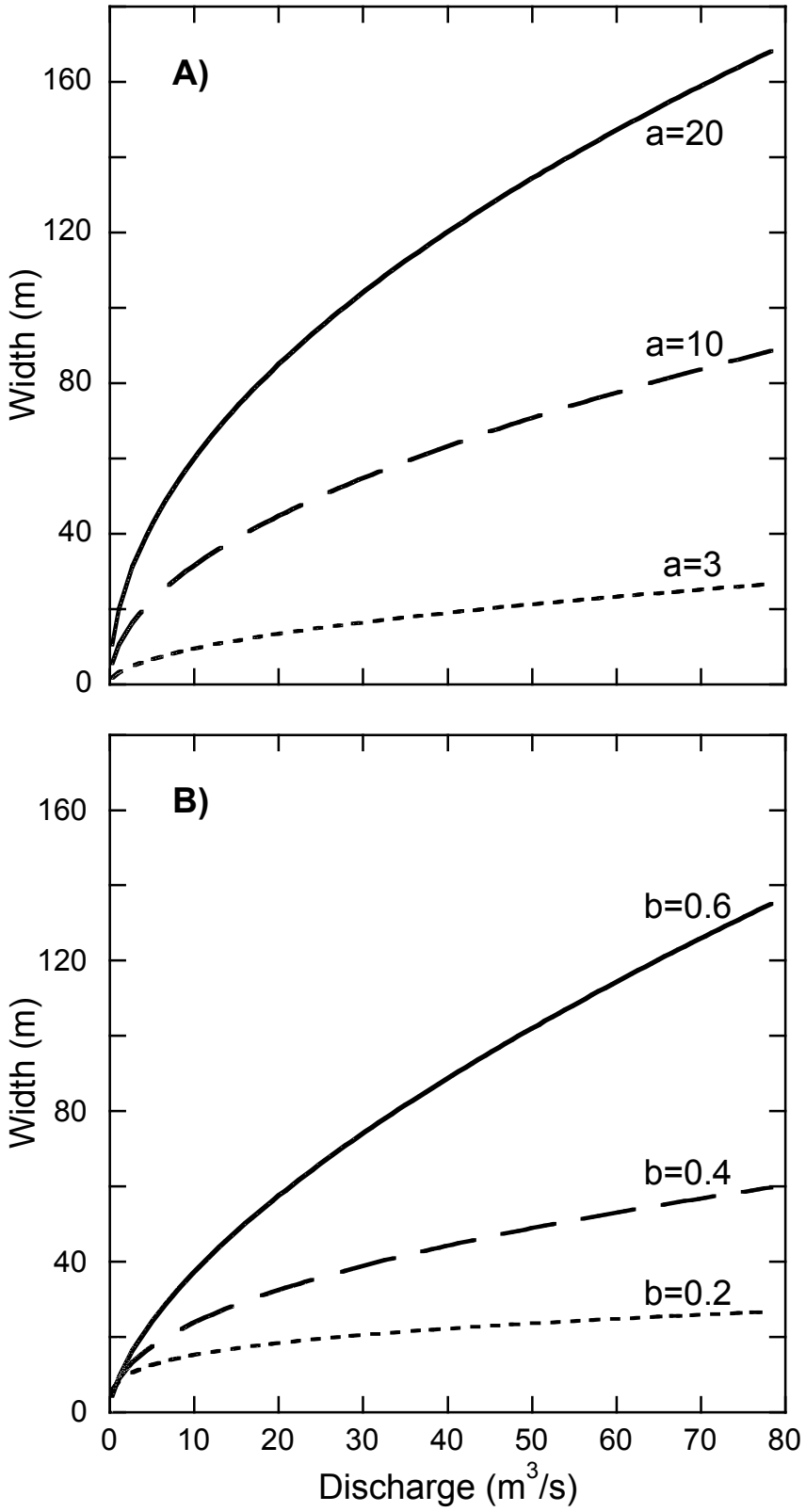
A)
a=20
a=10
a=3
Width (m)
0
40
80
120
160
B)
b=0.6
b=0.4
b=0.2
Width (m)
0
40
80
120
160
0
10
20
30
40
50
60
70
80
Discharge (m3/s)

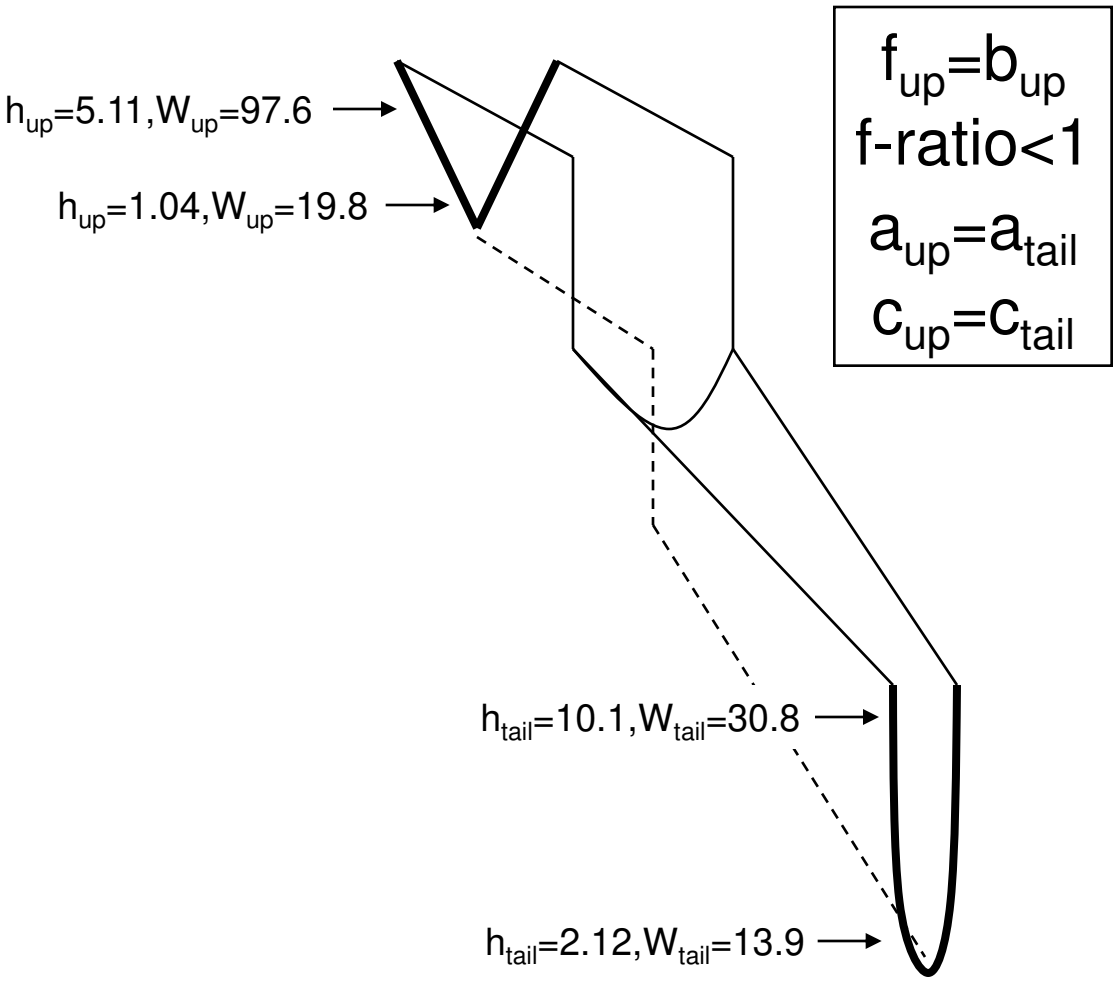
h_{up}=5.11,W_{up}=97.6
h_{up}=1.04,W_{up}=19.8
h_{tail}=10.1,W_{tail}=30.8
h_{tail}=2.12,W_{tail}=13.9
$f_{up}=b_{up}$
f-ratio<1
$a_{up}=a_{tail}$
$c_{up}=c_{tail}$

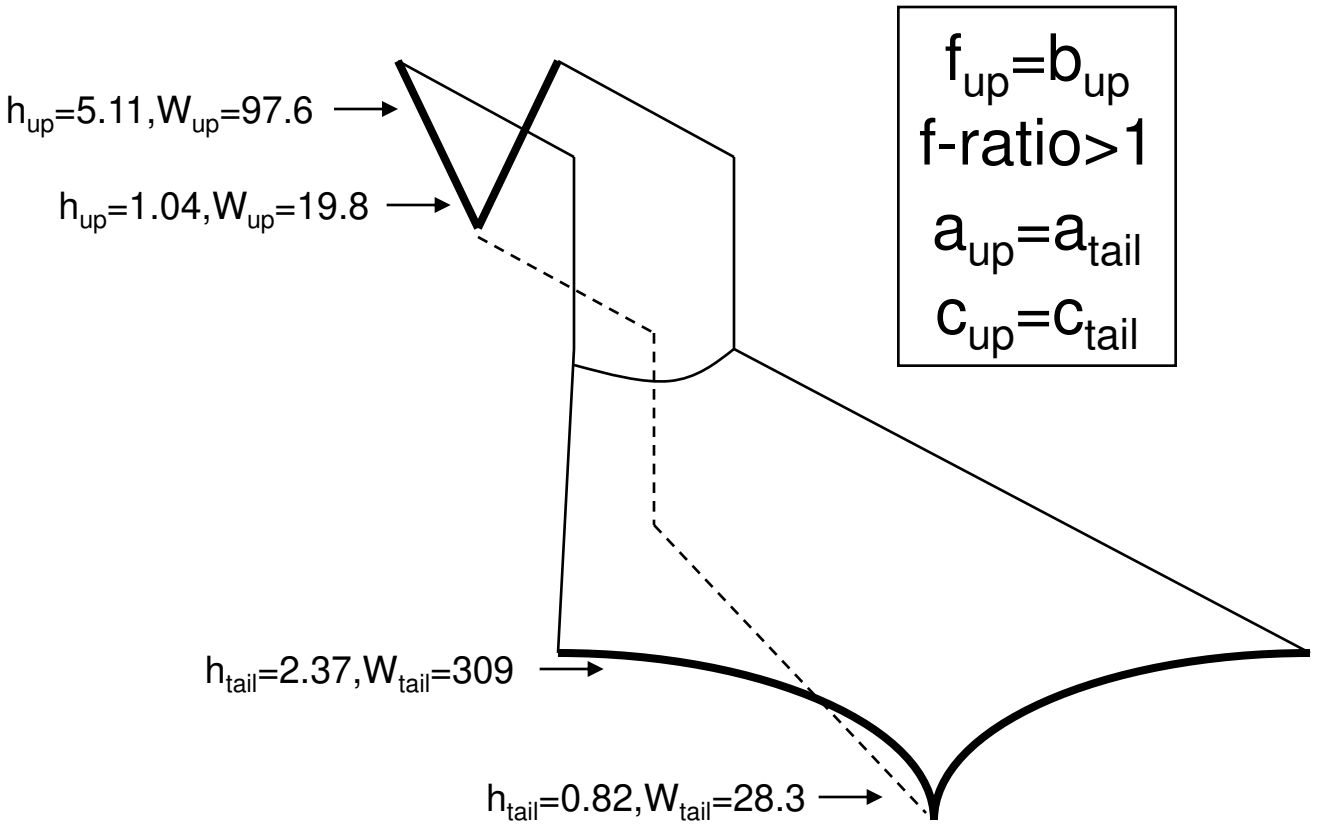
h_{up}=5.11,W_{up}=97.6
h_{up}=1.04,W_{up}=19.8
f_{up}=b_{up}
f-ratio>1
a_{up}=a_{tail}
c_{up}=c_{tail}
h_{tail}=2.37,W_{tail}=309
h_{tail}=0.82,W_{tail}=28.3

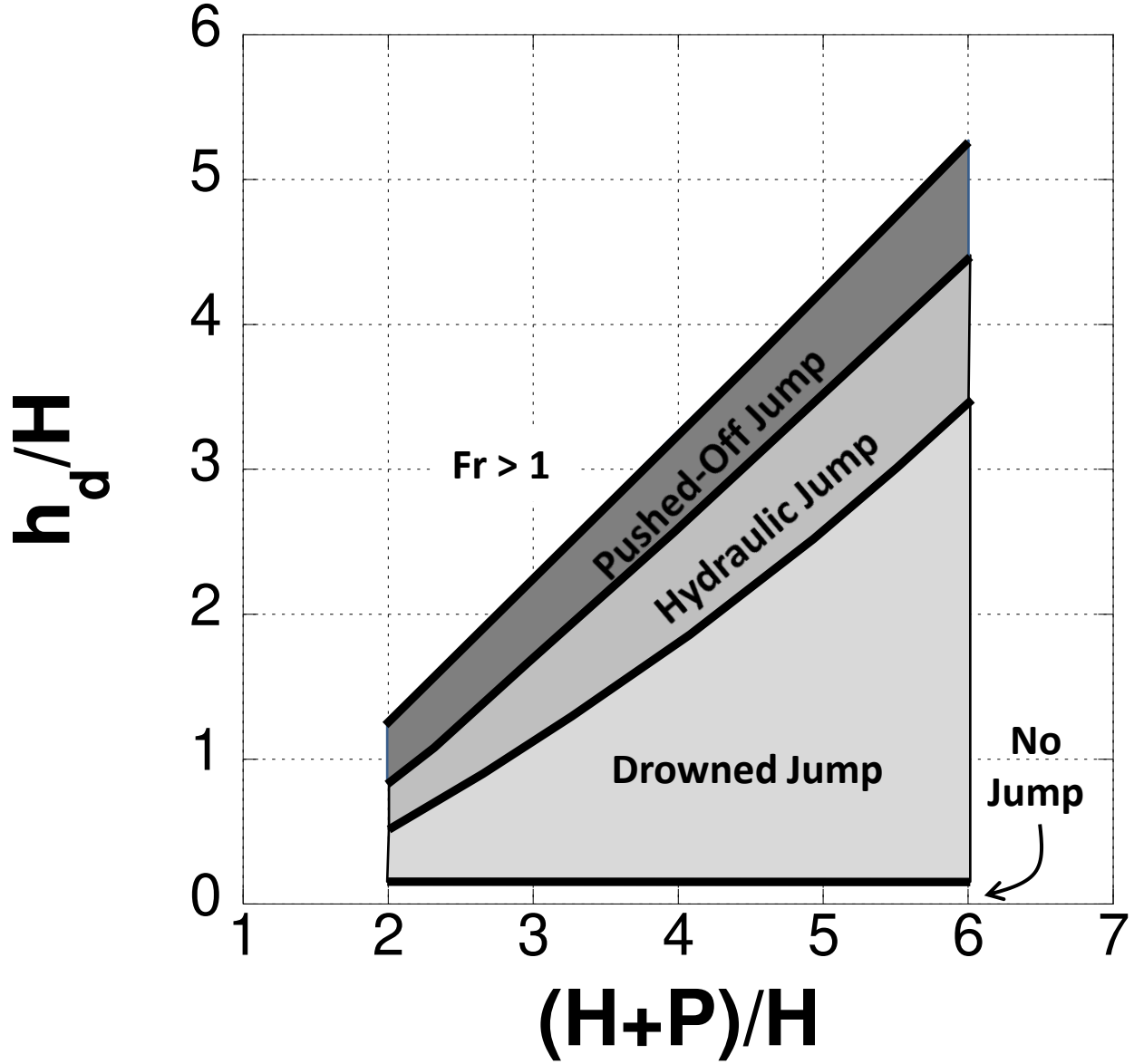
h_d/H
6
5
4
3
2
1
0
1
2
3
4
5
6
7
(H+P)/H
Fr > 1
Pushed-Off Jump
Hydraulic Jump
Drowned Jump
No Jump

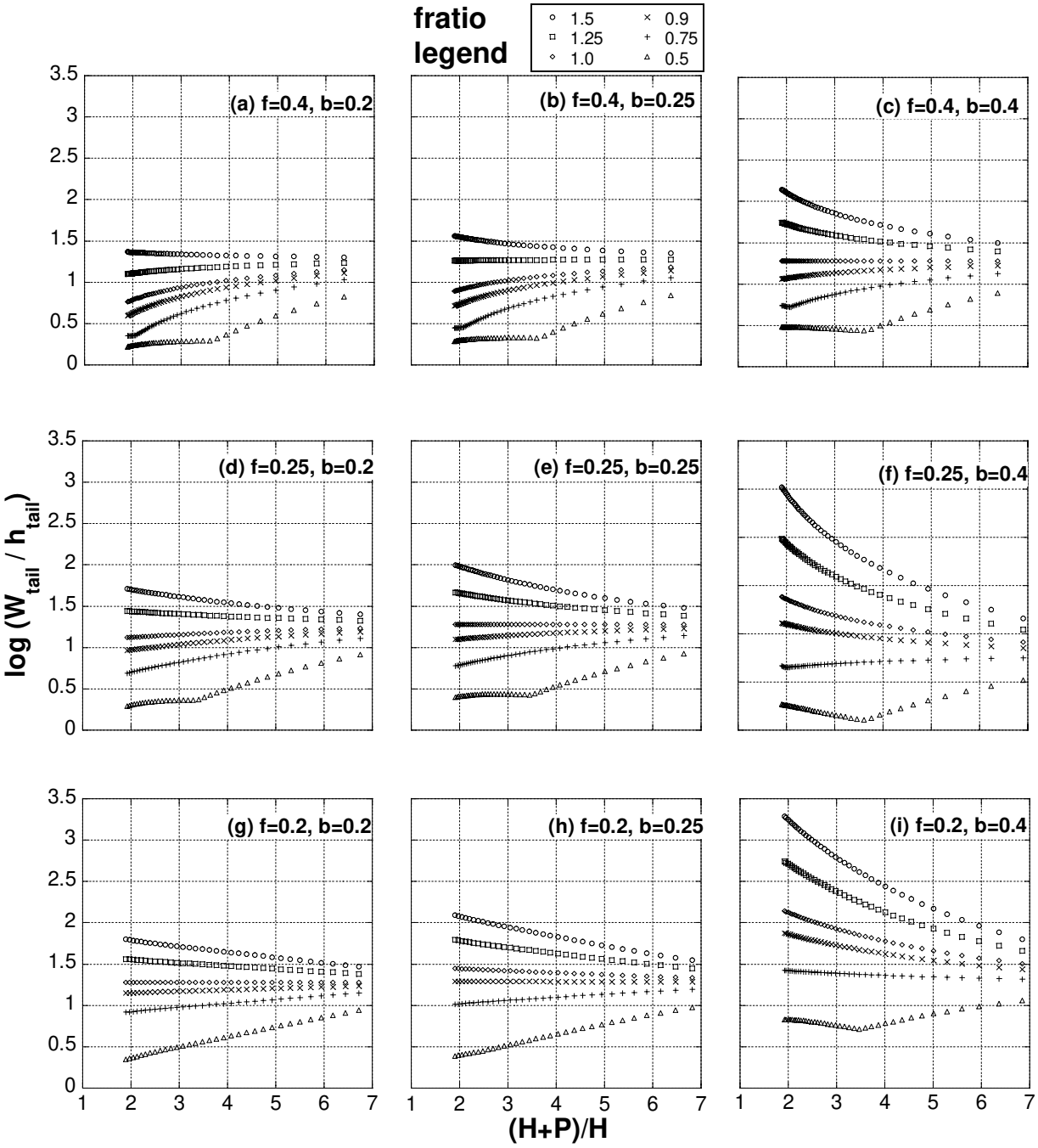
fratio legend
1.5
1.25
1.0
0.9
0.75
0.5
(a) f=0.4, b=0.2
(b) f=0.4, b=0.25
(c) f=0.4, b=0.4
(d) f=0.25, b=0.2
(e) f=0.25, b=0.25
(f) f=0.25, b=0.4
(g) f=0.2, b=0.2
(h) f=0.2, b=0.25
(i) f=0.2, b=0.4
log (W_tail / h_tail)
(H+P)/H

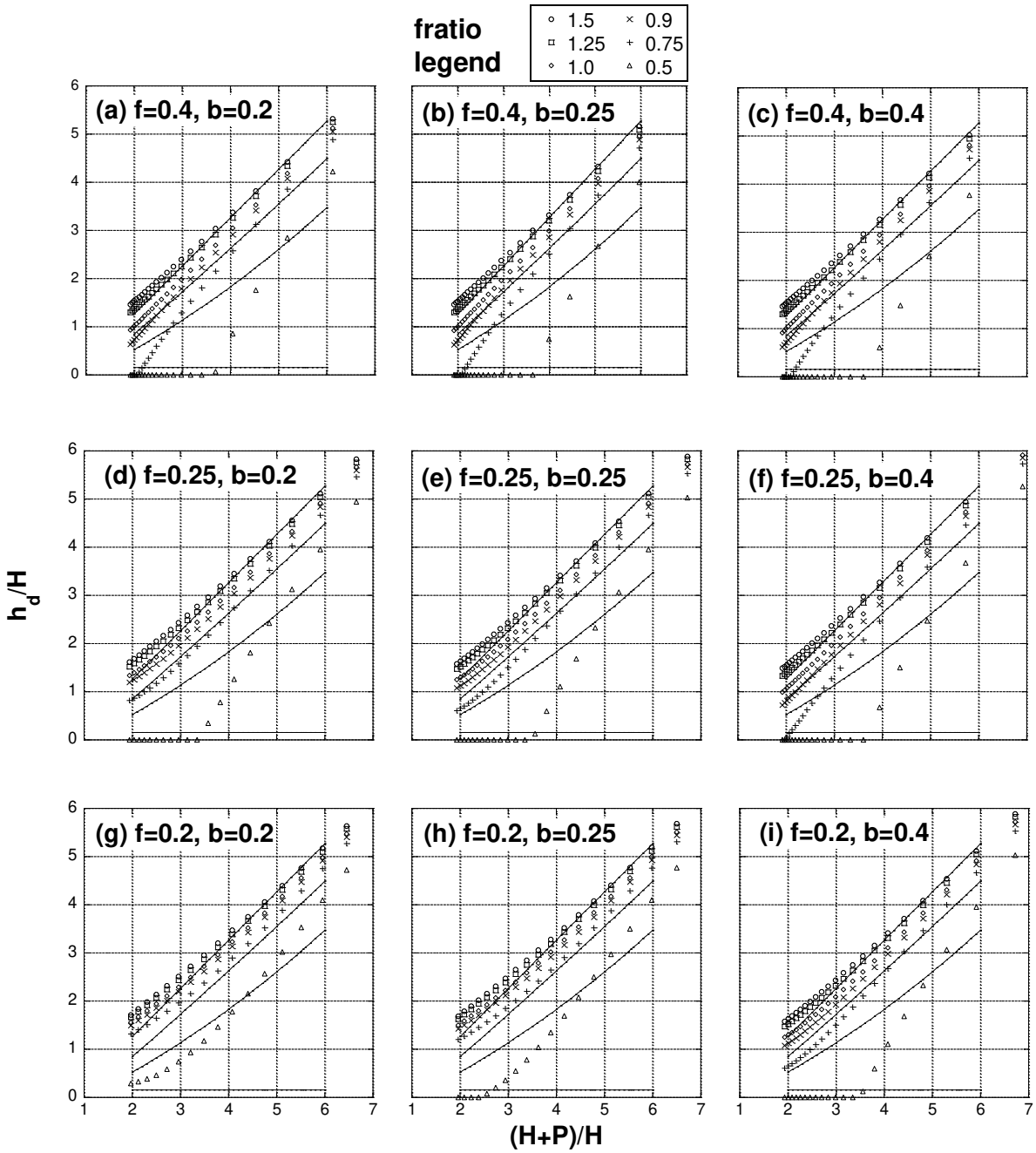
fratio legend
1.5
1.25
1.0
0.9
0.75
0.5
(a) f=0.4, b=0.2
(b) f=0.4, b=0.25
(c) f=0.4, b=0.4
(d) f=0.25, b=0.2
(e) f=0.25, b=0.25
(f) f=0.25, b=0.4
(g) f=0.2, b=0.2
(h) f=0.2, b=0.25
(i) f=0.2, b=0.4
h_d/H
(H+P)/H

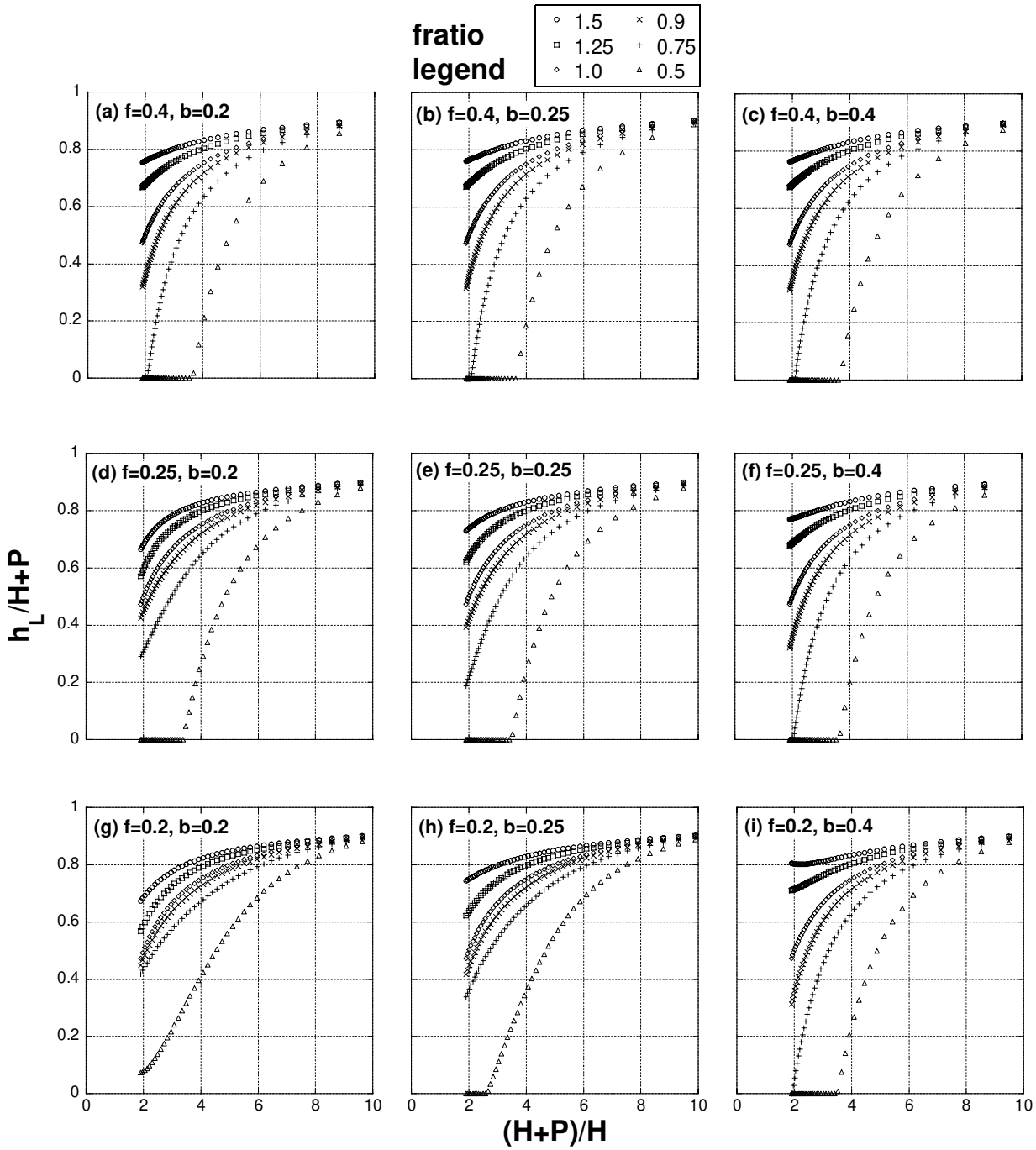
fratio legend
1.5
1.25
1.0
0.9
0.75
0.5
(a) f=0.4, b=0.2
(b) f=0.4, b=0.25
(c) f=0.4, b=0.4
(d) f=0.25, b=0.2
(e) f=0.25, b=0.25
(f) f=0.25, b=0.4
(g) f=0.2, b=0.2
(h) f=0.2, b=0.25
(i) f=0.2, b=0.4
h_L/H+P
(H+P)/H
0
0.2
0.4
0.6
0.8
1
0
2
4
6
8
10

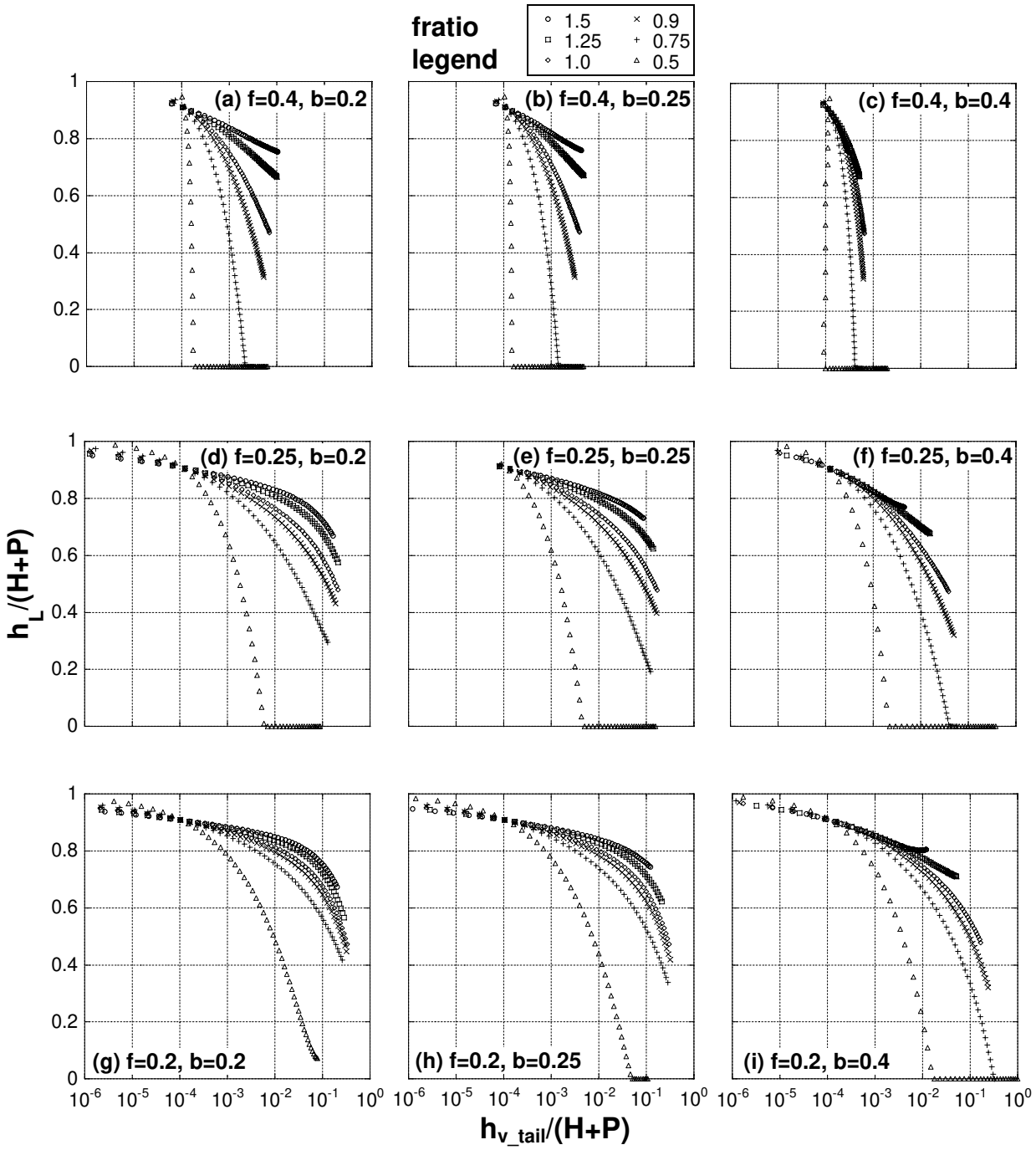
fratio legend
1.5
1.25
1.0
0.9
0.75
0.5
(a) f=0.4, b=0.2
(b) f=0.4, b=0.25
(c) f=0.4, b=0.4
(d) f=0.25, b=0.2
(e) f=0.25, b=0.25
(f) f=0.25, b=0.4
(g) f=0.2, b=0.2
(h) f=0.2, b=0.25
(i) f=0.2, b=0.4
h_L/(H+P)
h_v_tail/(H+P)
0
0.2
0.4
0.6
0.8
1
10^-6 10^-5 10^-4 10^-3 10^-2 10^-1 10^0

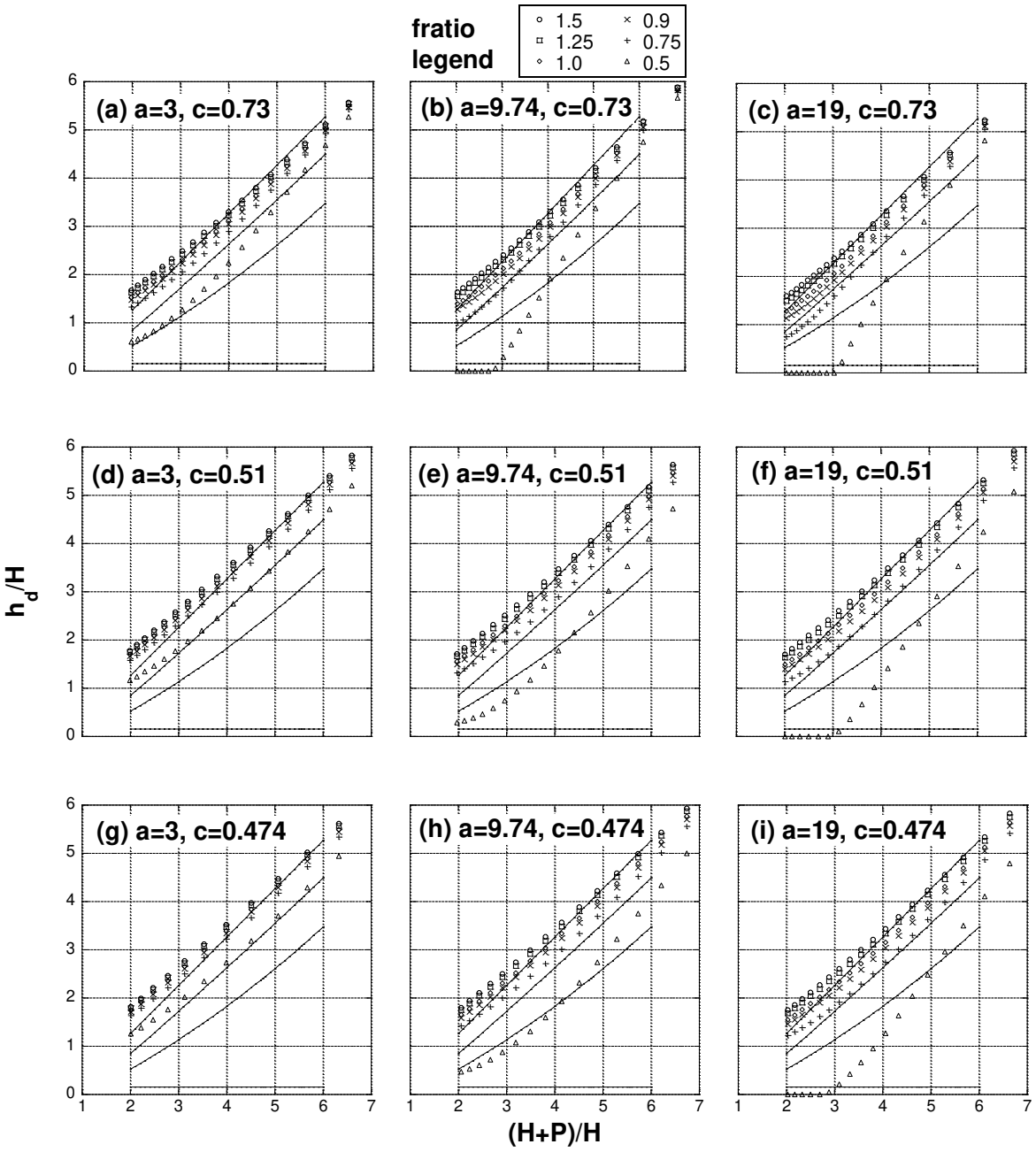
fratio legend
1.5
1.25
1.0
0.9
0.75
0.5
(a) a=3, c=0.73
(b) a=9.74, c=0.73
(c) a=19, c=0.73
(d) a=3, c=0.51
(e) a=9.74, c=0.51
(f) a=19, c=0.51
(g) a=3, c=0.474
(h) a=9.74, c=0.474
(i) a=19, c=0.474
h_d/H
(H+P)/H

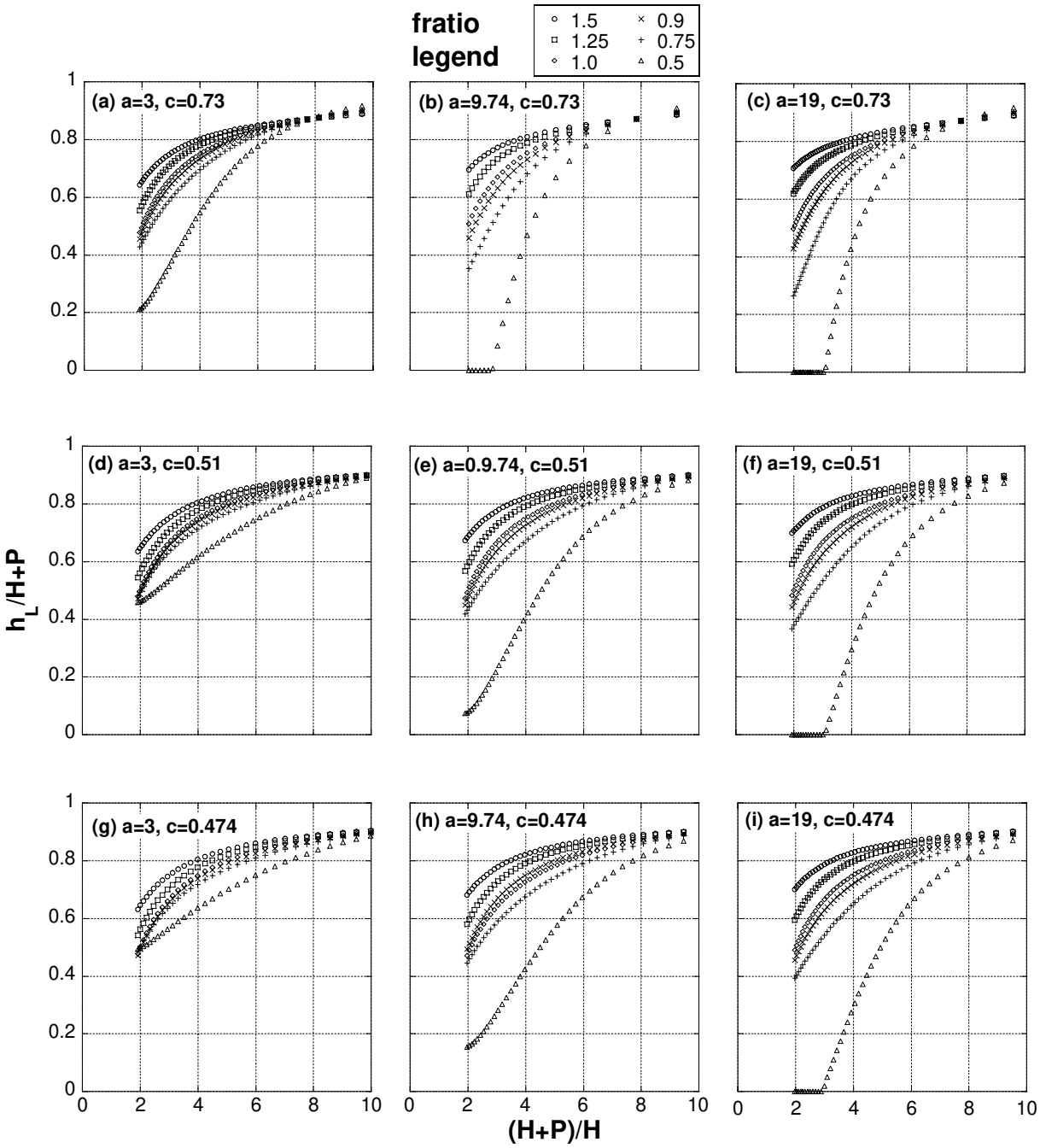
fratio
legend
1.5
1.25
1.0
0.9
0.75
0.5
(a) a=3, c=0.73
(b) a=9.74, c=0.73
(c) a=19, c=0.73
(d) a=3, c=0.51
(e) a=0.9.74, c=0.51
(f) a=19, c=0.51
(g) a=3, c=0.474
(h) a=9.74, c=0.474
(i) a=19, c=0.474
h_L/H+P
(H+P)/H
0
0.2
0.4
0.6
0.8
1
2
4
6
8
10

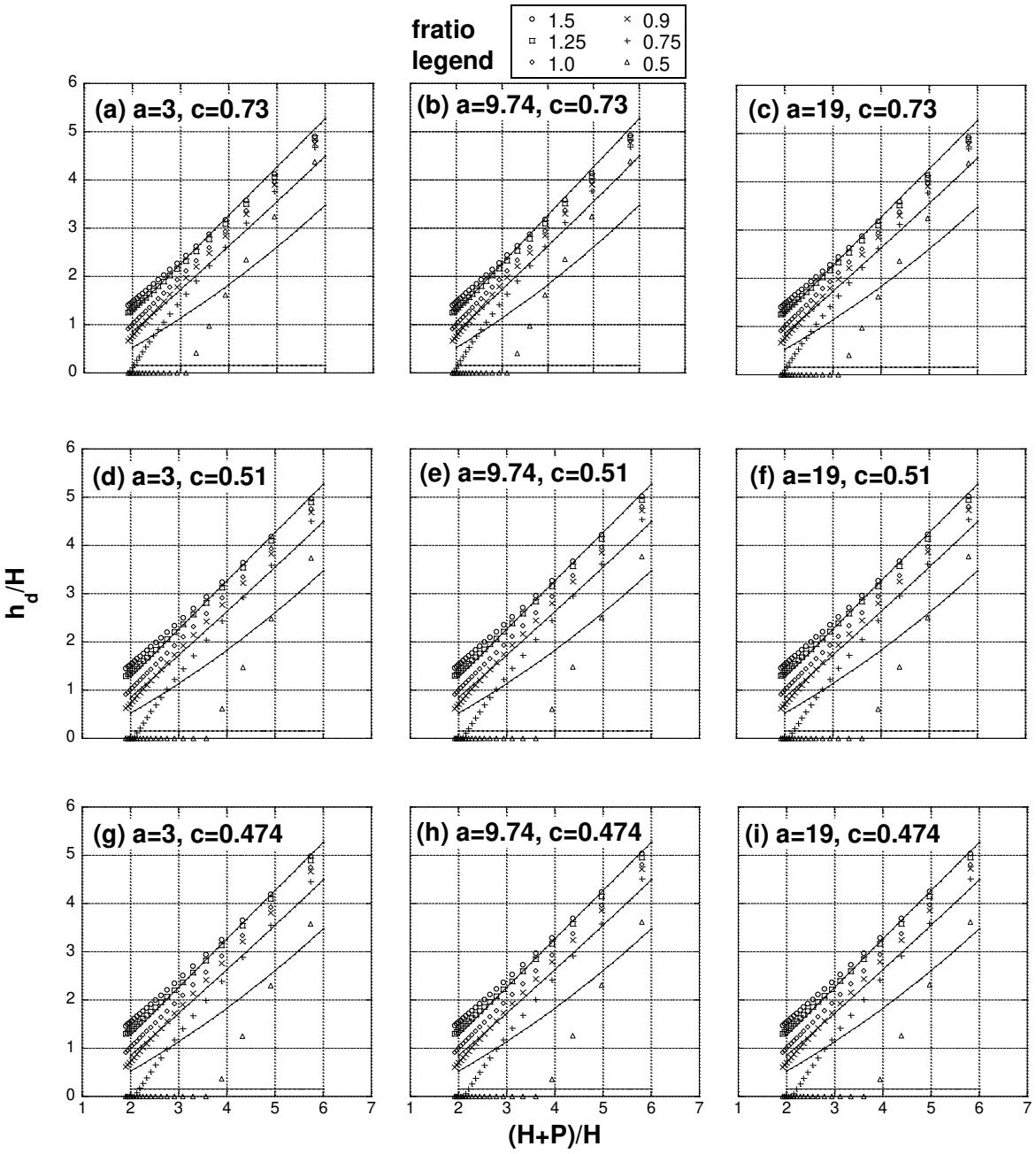
fratio legend
1.5
1.25
1.0
0.9
0.75
0.5
(a) a=3, c=0.73
(b) a=9.74, c=0.73
(c) a=19, c=0.73
(d) a=3, c=0.51
(e) a=9.74, c=0.51
(f) a=19, c=0.51
(g) a=3, c=0.474
(h) a=9.74, c=0.474
(i) a=19, c=0.474
h_d/H
(H+P)/H

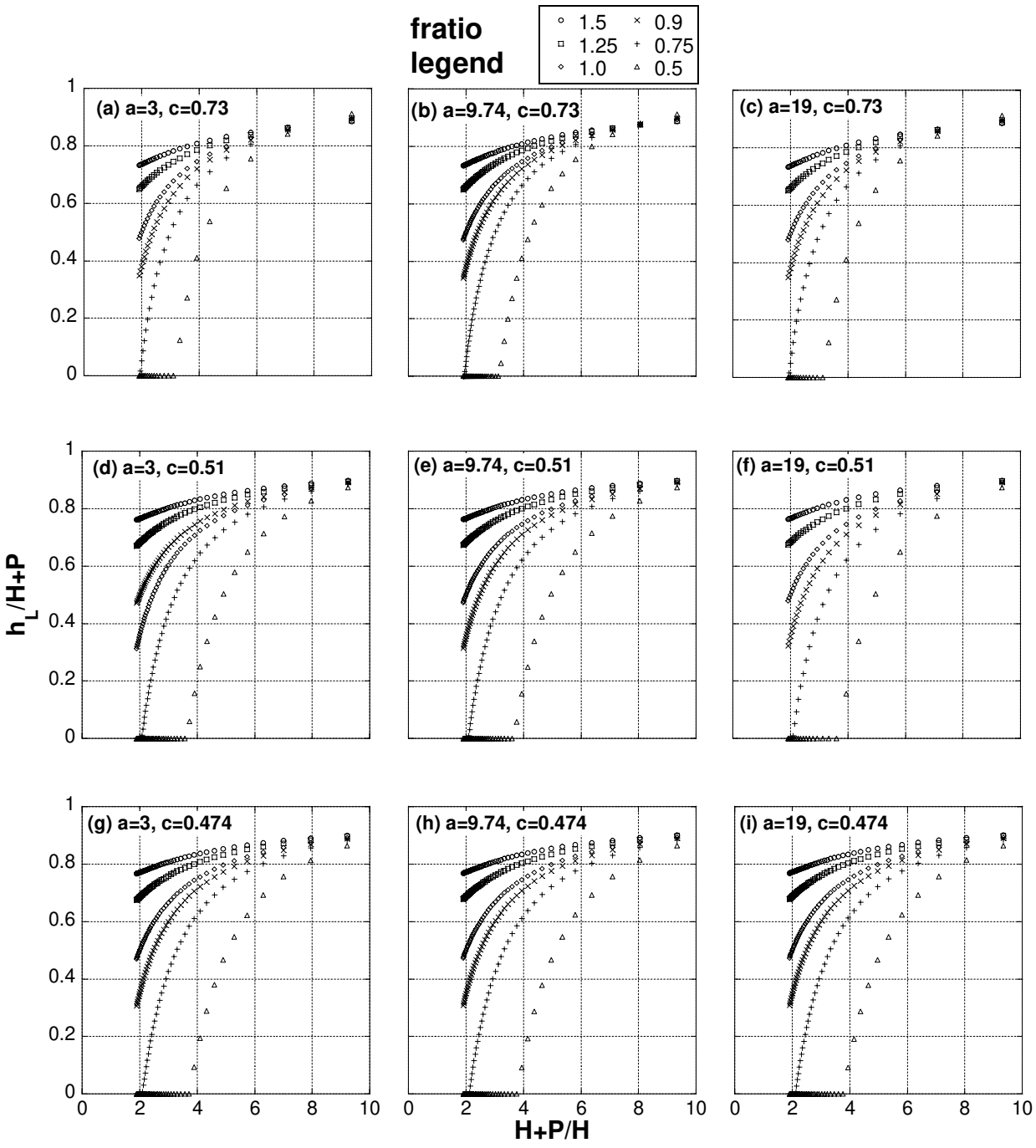
fratio legend
1.5
1.25
1.0
0.9
0.75
0.5
(a) a=3, c=0.73
(b) a=9.74, c=0.73
(c) a=19, c=0.73
(d) a=3, c=0.51
(e) a=9.74, c=0.51
(f) a=19, c=0.51
(g) a=3, c=0.474
(h) a=9.74, c=0.474
(i) a=19, c=0.474
h_L/H+P
H+P/H
0
0.2
0.4
0.6
0.8
1
0
2
4
6
8
10

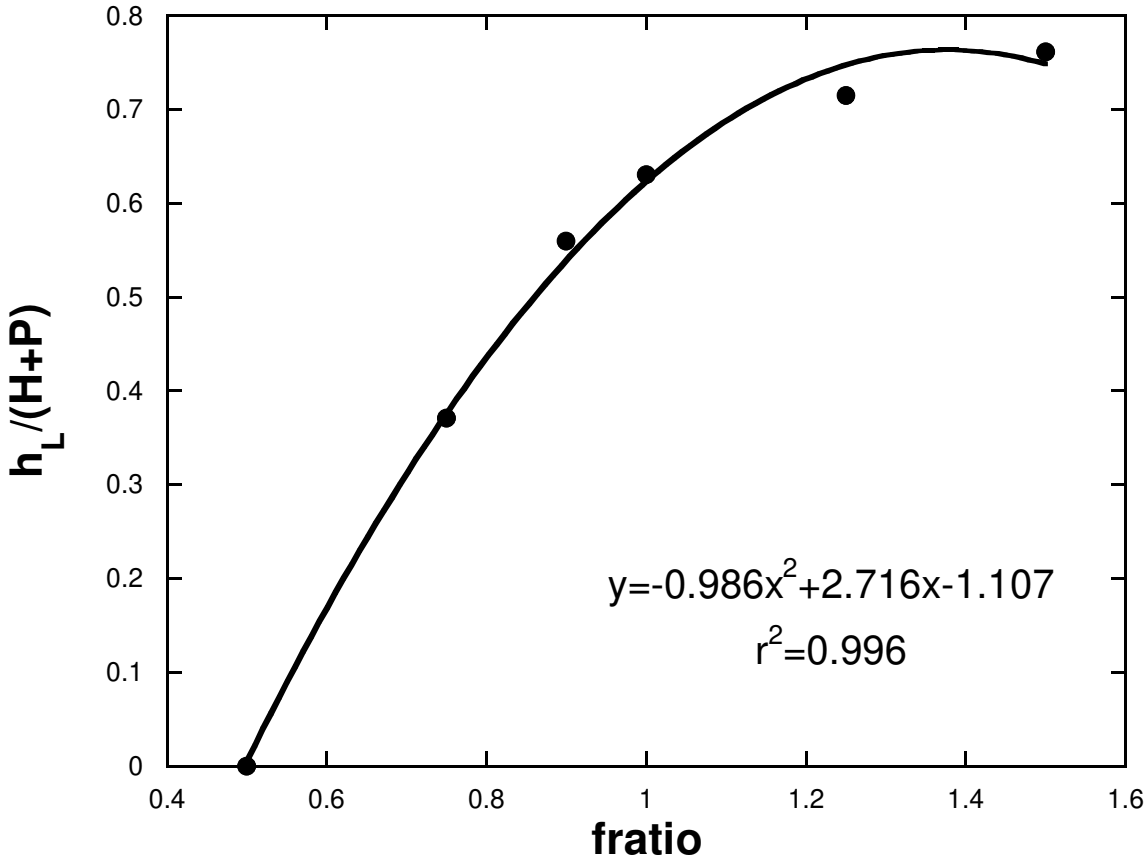
0.8
0.7
0.6
0.5
0.4
0.3
0.2
0.1
0
0.4
0.6
0.8
1
1.2
1.4
1.6
h_L/(H+P)
fratio
y=-0.986x^2+2.716x-1.107
r^2=0.996